

**Detecting and quantifying lake  
changes  
in the middle reaches of the  
Yangtze River over the last 70  
years (1945 – 2015)**

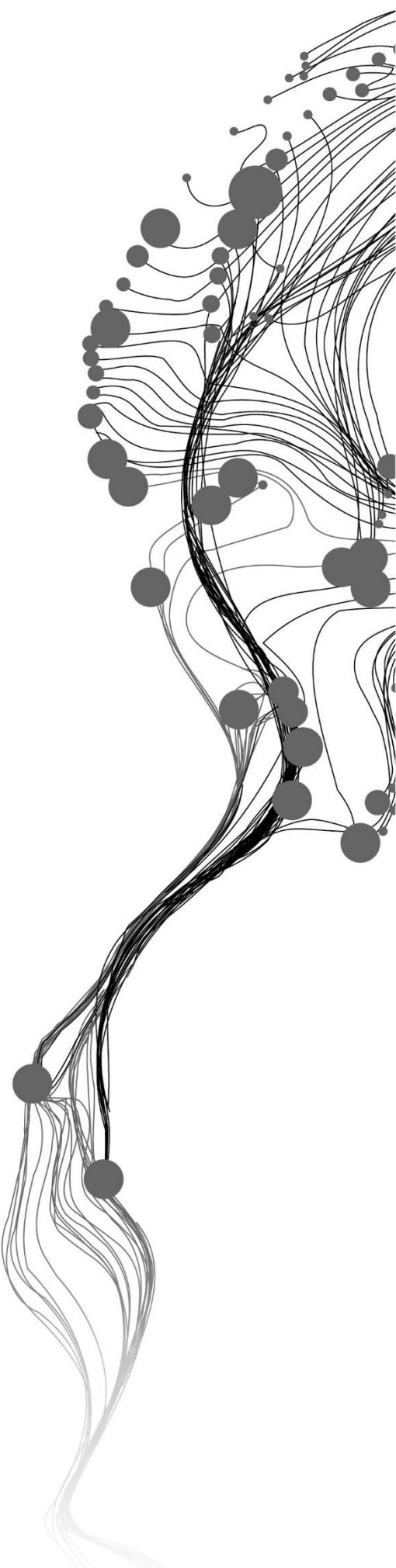
WEICHENG GENG

Enschede, The Netherlands, March, 2017

SUPERVISORS:

Dr. Tiejun Wang

Drs. Raymond G. Nijmeijer



# **Detecting and quantifying lake changes in the middle reaches of the Yangtze River over the last 70 years (1945 – 2015)**

**WEICHENG GENG**

Enschede, The Netherlands, March, 2017

Thesis submitted to the Faculty of Geo-Information Science and Earth Observation of the University of Twente in partial fulfilment of the requirements for the degree of Master of Science in Geo-Information Science and Earth Observation.

Specialization: Geographic Information for Natural Resource and Environmental Management

**SUPERVISORS:**

Dr. Tiejun Wang (ITC, University of Twente)

Drs. Raymond G. Nijmeijer (ITC, University of Twente)

**THESIS ASSESSMENT BOARD:**

Dr. Yousif A. Hussin (Chair)

Dr. Zoltan Vekerdy (External Examiner)

Dr. Tiejun Wang

Drs. Raymond G. Nijmeijer

#### DISCLAIMER

This document describes work undertaken as part of a programme of study at the Faculty of Geo-Information Science and Earth Observation of the University of Twente. All views and opinions expressed therein remain the sole responsibility of the author, and do not necessarily represent those of the Faculty.

## ABSTRACT

As the major component of wetland, lake plays a decisive role in ecological environment and human life. However, it is highly threatened by human activities. In China, there were a huge number of lakes vanished during last century, and the main cause is the rapid growth of economic and population. These changes mostly happened in the middle reaches of the Yangtze River, where exist the most abundant lake wetland resources. This study intends to detect and quantify the lake changes in the middle reaches of the Yangtze River over past 70 years. As one of the major urban agglomerations located in the middle reaches of the Yangtze River, Wuhan metropolitan area is the most representative.

In the study, the lake distribution in 1945 was extracted from a legacy map named *Hankou*, with object-oriented image analysis approach. Meanwhile, Landsat TM (1991) and OLI (2013) images have been collected for mapping the lake distribution in both rainy (wet) season and dry season. By incorporating this Landsat satellite image-derived lake distribution maps, together with legacy map-derived lake information, the lake changes during these time period were assessed. Subsequently, the driving force of lake changes have been also assessed through mapping the land cover in 2013, on the lake vanished area.

The study results indicated that over past 70 years, the total area of lakes in study area decreased 56%-58%. Meanwhile, the average area of lakes decreased, together with the rising number of lakes, appeared a fragmentation trend in lake distribution. However, there is no significant change on the river connectivity of lakes (open and closed lakes). The study also showed about 70% of the former lake area have been replaced by farm, and build-up area only takes 6%.

The study suggests that it is necessary to incorporate remote sensing techniques into the driving factor analysis of lake changes. Moreover, the integration of legacy map-derived information and satellite-derived information needs to be cautious with the asymmetric precision and accuracy between different data source. All in all, this study facilitates lake change detection and has important implications for the long-term and sustainable development of the middle reaches of the Yangtze River.

## ACKNOWLEDGEMENTS

I appreciate the opportunity of 18-month study in the faculty of Geo-Information Science and Earth Observation (ITC) of the University of Twente, which absolutely expanded my horizons, broadened and deepened my knowledge in the field of ecology, remote sensing and geographic information. At the time of finishing my thesis, I would like to express my gratitude to all the people who helped and supported me during this research.

First and foremost, I tender my deepest thanks to Dr. Tiejun Wang, my ITC supervisor, for introducing me such an interesting topic and teaching me how to conduct a scientific research independently. I have benefited a great deal from every discussion we had, and thanks very much for your advice and encouragement that cleared away my difficulties both in study and life.

My special thanks are addressed to Drs. Raymond G. Nijmeijer for removing so many obstacles to let me keep my mind on this research.

Finally, I would like to thank my parents for sparing no effort to support my study at ITC and this research.

# TABLE OF CONTENTS

---

1.	INTRODUCTION.....	7
1.1.	Background.....	7
1.2.	Problem statement .....	8
1.3.	Research identification .....	9
1.4.	Organisation of the thesis and research approach.....	10
2.	MATERIALS AND METHODS .....	13
2.1.	Study area.....	13
2.2.	Data preparation and pre-processing.....	16
2.3.	Methods .....	20
3.	RESULTS .....	27
3.1.	Distribution patterns of lakes in 1945 .....	27
3.2.	Distribution patterns of lakes in 1991 and 2013.....	28
3.3.	Change patterns of lakes over the last 70 years.....	29
3.4.	Driving factors of lake changes.....	36
4.	DISCUSSION.....	41
4.1.	Lake changes in the middle reaches of the Yangtze River over the last 70 years .....	41
4.2.	Driving factor of the lake changes .....	42
4.3.	Mapping the lake change maps and land cover maps.....	42
5.	CONCLUSION AND RECOMMENDATION .....	45
5.1.	Conclusions .....	45
5.2.	Recommendation .....	45

## LIST OF FIGURES

---

Figure 1 Framework of the research approaches.....	11
Figure 2 Location of the study area in Hubei province, China .....	13
Figure 3 Location of the study area in Hubei province along the Yangtze River. ....	14
Figure 4 The major cities and lakes along the middle reaches of the Yangtze River and the Three Gorges Dam. ....	14
Figure 5 scanned topographic map Hankou (left) and the reliability diagram (right).....	16
Figure 6 Sample plots of water presence and absence data used in the images in 1991(orange) and 2013(green).....	18
Figure 7 Calculated NDWI value image in the dry season of 2013.....	22
Figure 8 The threshold-based water extraction result of the NDWI image in the dry season of 2013, the threshold of this image has been set as 0.05.....	23
Figure 9 The post-processed water extraction map of the dry season in 2013, i.e. the final lake distribution of the dry season in 2013 .....	24
Figure 10 The open and closed lake distribution map of 1945, in which the Yangtze River have been showed only for reference. ....	27
Figure 11 The open and closed lake distribution map in 1991 wet season(left) and dry season(right), in which the Yangtze River and its branches have been showed only for reference.....	28
Figure 12 The open and closed lake distribution map in 2013 wet season(left) and dry season(right), in which the Yangtze River and its branches have been showed only for reference.....	28
Figure 13 The lake change map between 1945 and 1991 wet season (left) and dry season(right). The purple area on the maps could be considered as the vanished lake area. ....	29
Figure 14 The lake change map between 1945 and 2013 wet season (left) and dry season(right). The purple area on the maps could be considered as the vanished lake area. ....	29
Figure 15 Bar plot of the total area of lakes calculated from five lake distribution maps, with open and closed lakes separately. ....	30
Figure 16 Bar plot of the number of lakes calculated from five lake distribution maps, with open and closed lakes separately. ....	30
Figure 17 Bar plot of the total area of lakes calculated from five lake distribution maps, with open and closed lakes separately. ....	31
Figure 18 Bar plot of the largest lake patch size calculated from five lake distribution maps.....	32
Figure 19 Bar plot of the LSI calculated from five lake distribution maps. ....	32
Figure 20 The land cover map in 2013.....	36
Figure 21 The partial land cover map in which the lake vanished area from 1945 to 1991 wet season(left) and dry season(right).....	37
Figure 22 The partial land cover map in which the lake vanished area from 1945 to 2013 wet season(left) and dry season(right).....	37
Figure 23 The pie chart of the occupation rate of each class in each image from Figure 21 and 22. ...	38

## LIST OF TABLES

---

Table 1 Description of data used in this study and their usage. ....	19
Table 2 Defination of each land cover class in the land cover map 2013.....	25
Table 3 The statistical measurement indices used in the quantification assessment of lake changes in this study and their meanings.....	26
Table 4 Confusion matrix derived measures of classification accuracy and pairwise comparability..	26
Table 5 The landscape attribute of lakes in 1945, the dry season and wet season in 1991 and the dry season and wet season in 2013, and the decrease percentage from 1945 and 1991 in the last two rows .....	33
Table 6 The confusion matrix of the image classified by NDWI threshold in 1991 wet season presented by the number of pixels, with overall accuracy, estimate accuracy and Kappa coefficient in the last two rows. ....	34
Table 7 The confusion matrix of the image classified by NDWI threshold in 1991 dry season presented by the number of pixels, with overall accuracy, estimate accuracy and Kappa coefficient in the last two rows. ....	34
Table 8 The confusion matrix of the image classified by NDWI threshold in 2013 wet season presented by the number of pixels, with overall accuracy, estimate accuracy and Kappa coefficient in the last two rows. ....	34
Table 9 The confusion matrix of the image classified by NDWI threshold in 2013 dry season presented by the number of pixels, with overall accuracy, estimate accuracy and Kappa coefficient in the last two rows. ....	35
Table 10 The z-statistic comparing the confusion matrix of the four images classified by NDWI threshold.....	35
Table 11 The occupation area and rate of five classes on the former lakes area retrieved by lake change map between 1945 and the dry season in 1991, the wet season in 1991, the dry season in 2013, the wet season in 2013 respectively. ....	38
Table 12 The confusion matrix presented by the number of pixels of each class in the land cover map in 2013 with overall accuracy and Kappa coefficient in the last two rows. ....	39
Table 13 The producer's accuracy and user's accuracy of each class in the land cover map in 2013, with both the percentage of accuracy and proportion of pixels.....	39





# 1. INTRODUCTION

## 1.1. Background

Lake is usually defined as a basin with variable size of water which surrounded by land and apart from river. Usually, lake is larger and deeper than ponds, and different from river and stream with still water. There is no official or scientific definition of lake, and it could be part of wetland or artificial pond. In geologic time scales, all the lakes are temporary, which will slow filled by sediments or spill out of the basin. As an important part of wetland ecological landscape, lake provides a variety of ecosystem functions, ranging from flood control to nutrient retention and export (Groot, 2006). Artificial lakes could be sorted as industrial use, agricultural use, hydro-electric power use, domestic water supply and aesthetic or recreational use. As the major component of urban wetland (namely wetlands in urban area, including artificial wetlands, semi-artificial wetlands and remnant nature wetlands in urban construction), plays a decisive role in human production and life (Wang, Ning, Yu, Xiao, & Li, 2008). And at the same time, it is highly affected by human activities, driven by artificial factors and irreversible (Lemly & Ohlendorf, 2002). Currently, in the globe perspective, the biodiversity of lake ecosystems is threatened by nutrient load, contamination, acid rain and invasion of exotic species (Brönmark & Hansson, 2002; Fang et al., 2006). Also, the new threats such as global warming, ultraviolet radiation, endocrine disruptors and transgenic organisms especially happened in developing countries.

In China, there exist a large number of lakes provides enormous cultural and economic value. According to a survey in 1960-1980, there were 2928 lakes with an area more than 1 km<sup>2</sup>, which covering total 91019.6 km<sup>2</sup> area (Cui et al., 2013). For several decades, lake is always regarded as valuable resources and the conservation and protection has been a priority. However, during past 30 years, owing to economic growth, the conservation of lake lagged and lake area dwindled (Ma et al., 2011; Niu et al., 2012). The role lakes played in the middle reaches of the Yangtze River is especially vital. The middle reaches of the Yangtze River exist most abundant lake wetland resources and yet is the most serious wetland degradation area. As one of the core cities of this area, Wuhan has an alias called “River Town”, where exist a total of 138 lakes larger than 0.1 km<sup>2</sup> and 20% of them in the main city areas until 2003 (Xu et al., 2010). However, in recent years, due to population explosion and rapid development of the economy, overexploitation of the urban areas like filling lake to build house has taken place in Wuhan, result in the shrinkage of water areas and quality (Xu et al., 2010). The ecological function of lakes has been affected, and the flood control capacity has been damaged as well. It means the flood prevention and mitigation ability has been impaired. In fact, inundation and flood incident is increasing recent years(Deng, 2006).

As the main driven force, human activity affects lake changes in both direct and indirect aspect. Although changes in lake happen in natural, the trend and purpose have been changed by various human activities. Urban expansion supposed to be the main causes from human and could affect landform in short period (D. Jiang, Fu, & Wang, 2013). In particular area and period this phenomenon especially obvious. In China, driven by the policy of economic reform and the market economy in 1978, the gross domestic product (GDP) of the Yangtze River Basin rapidly increased. The average annual growth rate of GDP exceeded 10%. Wuhan is one of the major cities located in the Yangtze River Basin who driving China’s economic growth and influence the overall pattern of regional development in China. The rapid urbanisation and industrialisation in the Yangtze River Basin caused a series of problems due to the long-term absence of a strong overall develop plan, and disordered territorial development as well (Tang, Fan, & Sun, 2015). In 2010, Xu et al. produced the urban wetlands change map from 1987 to 2005 by land use maps, and the

results showed nature wetlands trend to become artificial wetland. Meanwhile, the lake wetland area of Wuhan declined due to fragmentation. Similarly, a longer time range wetland dynamic changes mapping focused on one of the largest lakes in Wuhan city, Tangxunhu wetland, have been studied by Xu et al. (2009). Retrieving cartography and statistical assessment from 1953 to 2005, in which land use and water indices showed Tangxunhu wetland was very unstable and its structure becomes more complex. The study suggested Tangxunhu wetland affect more influence from human during 1953 to 1967 than the period from 1967 to 2005. The influences from human including reclamation, aquaculture and pollutants, not only by modification of the wetland itself, but also by adjacent land use (Burbridge, 1994; Detenbeck, Taylor, Lima, & Hagley, 1995). In 2008, Wang et al. also give a study showed urban construction induced damage on wetland in 1996-2001, these damages include the decline of lake area and fragmentation degree of all wetland.

The development of satellite remote sensing based techniques has offered opportunities for monitoring in many aspects, ranging from the spatiotemporal views to feature views such as the transparency, biota and ice phenology (Dörnhöfer & Oppelt, 2016). Data from different sensors could provide water information in various scale and aspects. The radar laser altimeters could provide the elevation of water thus calculate the volume of water body (Huang, Peng, Lang, Yeo, & McCarty, 2014). Airborne sensors could collect the hyperspectral image of water surface for aquatic vegetation and cyanobacteria estimation (Chipman, J.W., 2009). In 2015, Gao provided a comprehensive review of lake area estimation through satellite remote sensing approaches. The algorithms which employ visible and infrared bands for detecting water could be sorted in threshold-based approaches and image classification-based approaches. The image classification-based approaches are represented by the supervised and unsupervised image processing algorithms, and the threshold-based approaches through adopt thresholds from the radiative properties of spectral water indices. Water Indices are often used to mapping open water body with user-defined threshold, including Normalized Difference Water Index (NDWI), Automated Water Extraction Index (AWEI), Water Index (WI) and Simple Water Index (SWI) (H. Jiang et al., 2014; Malahlela, 2016), etc. Among the various indices, several forms of the Normalized Difference Water Indices (NDWIs) are often preferred over other indices (Sun, Sun, Chen, & Gong, 2012). Rokni, Ahmad, Selamat, and Hazini (2014) suggests the NDWI performs better than other indices when the research involves spatiotemporal changes.

## **1.2. Problem statement**

To build knowledge about the long-term changes in the middle reaches of the Yangtze River now become more important. As the environment problem been highly regarded by local government and environmental organizations, to analysis and comprehend the long-term historical changes in the middle reaches of the Yangtze River will contribute to human in many aspects, including the conservation of the Yangtze River, protection of the ecological environment along the Yangtze River and sustainable development of the middle reaches of the Yangtze River.

Nowadays the technique of mapping lake changes is no longer a difficult problem, and more satellite images become open access and free for charge. Some research has been carried out focused on the lake changes in the middle reaches of the Yangtze River or the Wuhan city, but most of them only discussed the changes in recent decades in which available satellite images exists. However, the rapid lake changes happened in the middle reaches of the Yangtze River started from the early days when the establishment of People's Republic of China (PRC), which date back to the end of the 1940s. As the most accurate map we can find, the topographic map of Hankou covers four cities in the middle reaches of the Yangtze River, provides clear lake distribution information in 1945. It perfectly filled the vacancy of information in the early days of PRC's establishment.

As a complement to previous research, this research intends to map the changes of lakes over past 70 years in the middle reaches of The Yangtze River. Take advantage of topographic map in 1945 and Landsat satellite images. An overview of lake changes has been mapped, and its driving force has been analysed through land cover change map. Conventional water change detection techniques have been applied in this case and the driving force analysis has been implemented through the land cover map, which could show readers current land use types in the area lakes diminished. In addition, the water level difference between wet and dry season have been considered respectively. Meanwhile, as an important flood prevention factor, the river connectivity of lakes has been taken into account.

### **1.3. Research identification**

#### **1.3.1. Research objectives**

This research aims at detecting and quantifying lake changes in the middle reaches of the Yangtze River over the past 70 years (1945 – 2015) using historical topographic map and satellite imagery. To achieve this objective, there are four specific objectives:

1. To digitise and quantify the lakes in the middle reaches of the Yangtze River from the historical topography map generated in 1945, using object-oriented classification techniques.
2. To map the lakes along the middle reaches of the Yangtze River using multi-temporal Landsat satellite images in the 1980s and 2015, respectively.
3. To quantify lake change patterns (e.g., lake size, the number of lakes, and their connectivity to the Yangtze River) over the past 70 years (1945 – 2015) using spatial analysis techniques.
4. To identify and quantify the main driving factors behind the observed lake changes.

#### **1.3.2. Research questions**

1. What are the distribution patterns of lakes (e.g., lake size, the number of lakes, and their connectivity to the Yangtze River) in the middle reaches of the Yangtze River in 1945?
2. What are the distribution patterns of lakes (e.g., lake size, the number of lakes, and their connectivity to the Yangtze River) in the middle reaches of the Yangtze River during the flood and non-flood seasons in the 1980s and 2015, respectively?
3. What are the change patterns of lakes in the middle reaches of the Yangtze River over the past 70 years?
4. What are the main driving factors (i.e., human activities) responsible for the lake changes in the middle reaches of the Yangtze River?

#### **1.3.3. Research hypotheses**

Hypothesis 1

$H_0$ : There is no significant decline and fragmentation of lakes (i.e., lake size, the number of lakes, and their connectivity to the Yangtze River) in the middle reaches of the Yangtze River over the last 70 years.

$H_1$ : The lakes (i.e., lake size, the number of lakes, and their connectivity to the Yangtze River) in the middle reaches of the Yangtze River have been significantly declined and fragmented over the last 70 years.

## Hypothesis 2

$H_0$ : Urban expansion is not the main driving factor responsible for the lake decline and fragmentation in the middle reaches of the Yangtze River.

$H_1$ : Urban expansion is the main driving factor responsible for the lake decline and fragmentation in the middle reaches of the Yangtze River.

### **1.4. Organisation of the thesis and research approach**

This thesis constructed as followed structure. Chapter 1 summarises a general situation of research background, explains the research problem, defines the research objectives, questions and hypotheses, describes the general outline of the research. Chapter 2 introduces the study area, lists the data used in this research and the pre-processing of data, introduces the methods and accuracy assessment approach of classification result, narrates the research experimental process. Chapter 3 describes the output. Chapter 4 discusses results relevant to specific research hypotheses states in Chapter 1, and the methods and approaches involved in this research and the practical relevance of the results and implications. Chapter 5 concludes and summarises the research purpose and respected outcome and makes recommendation for further studies.

Followed flowchart demonstrates the overall framework of the research approaches. This research composed by two part of analysis, respectively corresponding to two hypothesis states in Chapter 1, namely mapping lake changes and driving factor analysis. In the first part, lake distribution in different time periods was derived by Object-oriented classification and NDWI threshold classification approaches and made the comparison. The latter part classified land cover in 2013, intended to analysis the driving factor of lake changes through land cover type. Relevant accuracy assessment result was interpolated in respective experimental section.

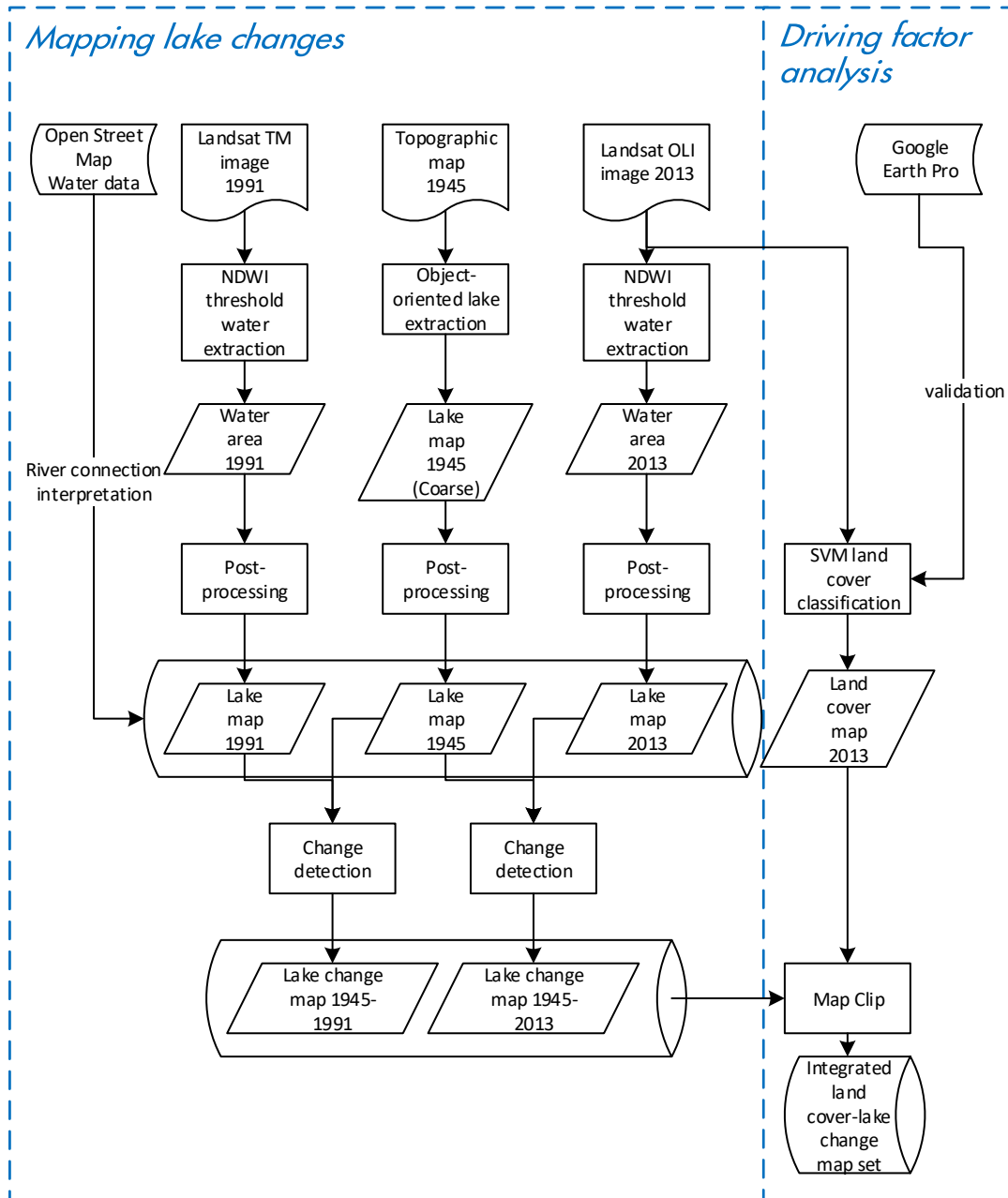


Figure 1 Framework of the research approaches.



## 2. MATERIALS AND METHODS

### 2.1. Study area

The study area in this study is based on the extent of topographic map in 1945. The geographical extent of the study area is  $114^{\circ}00' - 115^{\circ}30'$  E,  $30^{\circ}00' - 31^{\circ}00'$  N, covering an area of 14,100 km<sup>2</sup>. The study area covers four major cities of Wuhan metropolitan area, respectively are Wuhan, Huangshi, Huanggang and Ezhou.

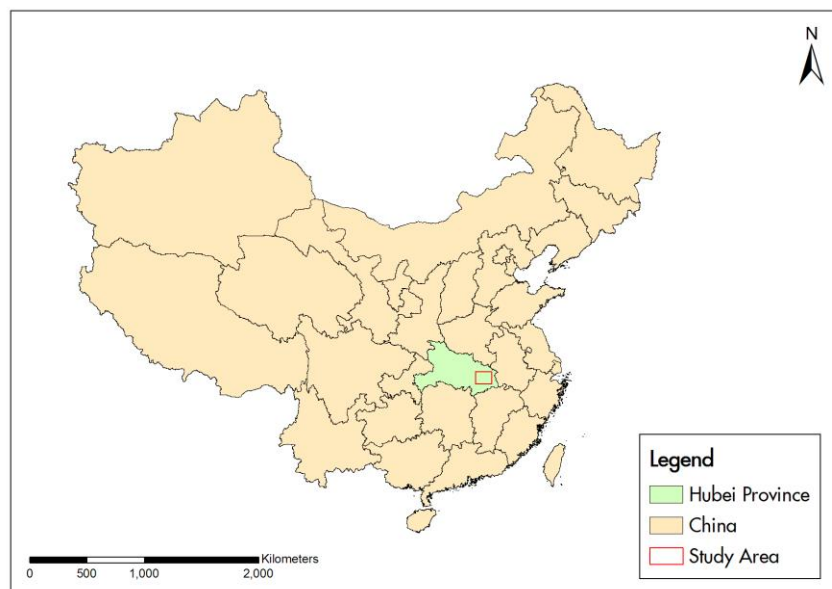


Figure 2 Location of the study area in Hubei province, China.

#### 2.1.1. The middle reaches of the Yangtze River

The Yangtze River, also known as the Chang Jiang or the Yangtze River Jiang, is the longest river in China and the third-longest in the world. It plays a key role in the social and economic development in China. Along the Yangtze River there exist many lakes which play important roles in water resource supply and flood control, also it provides habitats for many rare or endangered migratory birds.



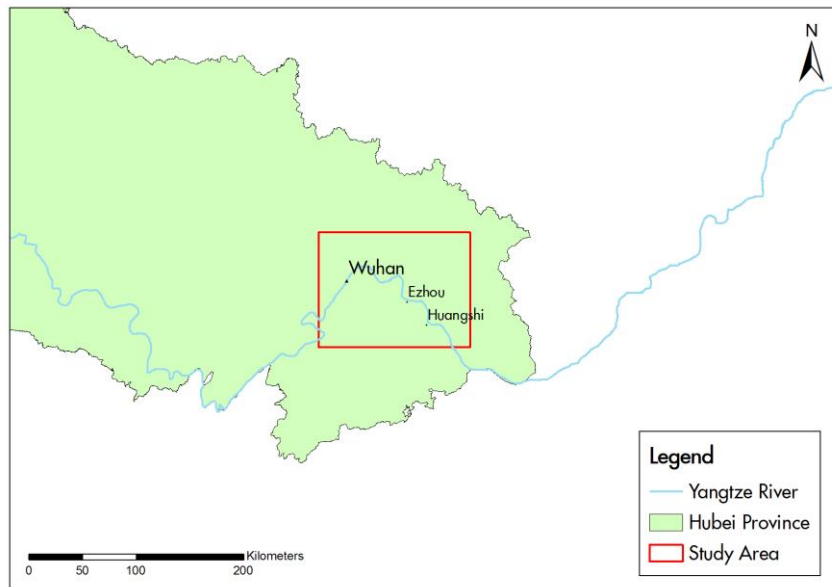


Figure 3 Location of the study area in Hubei province along the Yangtze River.

Wuhan metropolitan area located in the middle reaches of The Yangtze River, which is one of the largest urban agglomerations in this area. The landform types of Wuhan metropolitan area belong to alluvial plain of rivers and lakes, with a large number of rivers and lakes. Elevation in this region is less than 50m. The climate of this region belongs to semitropical monsoon climate, which shows a clear difference in four seasons and abundant precipitation during June to August. The mean annual temperature in this area ranges from 14 to 18 °C, and the average annual precipitation is approximately 1,300 mm.



Figure 4 The major cities and lakes along the middle reaches of the Yangtze River and the Three Gorges Dam.

### **2.1.2. Lakes in the middle reaches of the Yangtze River**

Located in the middle reaches of The Yangtze River, study area in this research have abundant wetland resources and most representative fresh lakes in China. Meanwhile, the study area is one of the most important agricultural and industrial regions in China. During past century, taking advantage of its geography location and natural resource, this region experienced rapid social and economic growth. However, with rapid socioeconomic development, half of the lakes in this area disappeared because of reclamation over past 70 years. Serious ecological and environmental problems have been caused, such as the capability of flood decreased, both quantities and quality of lake water declined, ecosystems have been damaged.

### **2.1.3. Flood and non-flood seasons**

As an important factor in water mapping, the variation of water level between wet seasons and dry seasons need to be taken into consideration. The water level of The Yangtze River changes significantly between wet and dry season. Lakes connected to The Yangtze River usually have significant water level variation among summer and winter (Cui et al., 2013). While in this study, the scanned map in 1953 cannot provide the specific date when aerial photo acquired. For this reason, the change detection needs to be performed on both dry and wet season, to show the possible maximum and minimum changes in the lake area. This study will use images from the local dry season (September to January in the next year) and wet season (June to August) in the 1980s and 2010s.

## 2.2. Data preparation and pre-processing

### 2.2.1. Historical topographic map

As the key data of this research, the scanned topographic map named *Hankou* is prepared by the Army Map Service (NSCOL), Corps of Engineers, Washington, D. C. Compiled in 1953 from the best available large scale maps of China. Planimetric detail partially revised by photo-planimetric methods from 1945 aerial photography, the revised area covered about half of the map, showed as reliability diagram (Figure 5). This map has been scanned in 37\*37 m<sup>2</sup> resolution.

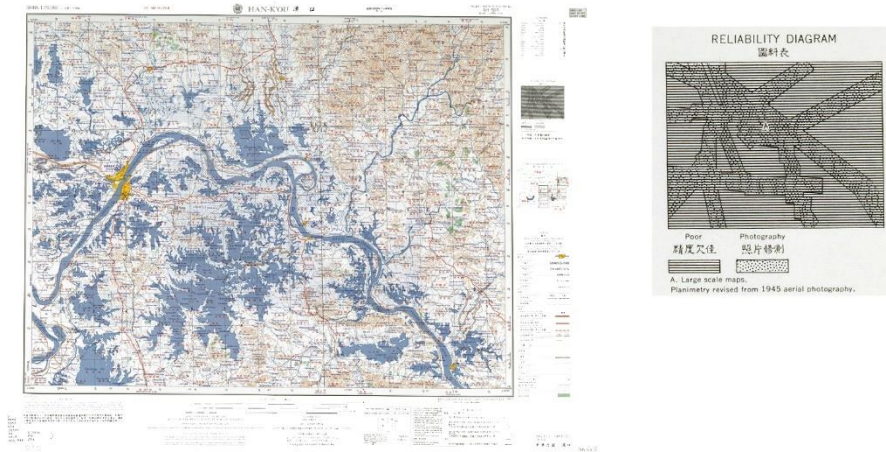


Figure 5 scanned topographic map *Hankou* (left) and the reliability diagram (right).

### 2.2.2. Landsat satellite imagery

Landsat TM was selected to extract lake information in the 1990s, and two aspects have been taken into account to made this selection. Due to the data availability, namely only limited images data in the early 1990s exists online, as one of the easiest accessible data sources, Landsat TM image could meet the requirement in this research which need to identify the lakes area accurately. To acquire the lake distribution information and land cover information is required in current years (the 2010s), Landsat OLI image was selected to extract these two kinds of information. For water extraction aspect, Landsat OLI sensor has near band composition with Landsat TM image, as well as the bandwidth and resolution. For land cover mapping aspect, Landsat OLI image provides six bands in 30 meters' resolution including visible spectrum and infrared bands, which could meet the requirement in the precision of land cover map.

To cover the entire study area, two scenes of image was used for this study both from Landsat TM sensor and Landsat OLI sensor. According to the WRS-2 system, the image from path 122, row 39 and path 123, row 39 was used for this research.

All the existing available Landsat TM images in the study area at the 1990s have been downloaded and checked. After excluding the images with cloud cover mostly on the top of the study area, two scenes of image from near acquired date covering study area have been selected for both wet and dry season. Four images in 1991 finally selected since a limited number of images meet the need, with the serial number 200, 209, 273 and 280. The Landsat OLI images in recent years need to be collected for water extraction and land cover classification using, considering the data availability, cloud cover, and also two scenes of images need to be acquired on near date. Finally, the images from dry and wet season in 2013 have been selected for this study, with the serial number 205, 212, 276 and 285.

The Landsat image data in this study downloaded from U.S. Department of the Interior U.S. Geological Survey (“USGS.gov,” 2016). Image from both TM and OLI sensors have been pre-processed in Precision and Terrain Correction (Level-1T, L1T) level, which provide geometric RMSE less than one pixel in 99.5 percent of Landsat 4-5 TM data and RMSE less than one pixel in 99.6 percent of Landsat 8 L1T data (“Landsat Missions,” 2017).

Downloaded satellite image data have been pre-processed in ENVI software by following steps: radiometric calibration, Quick Atmospheric Correction (QUAC), image mosaicking and resize. First, in radiometric calibration, images were converted from digital number (DN) value to top-of-atmosphere (TOA) reflectance using Landsat Calibration tool. Second, the QUAC module provided in ENVI was used to reduce the effect of the atmosphere. On account of images acquired date and data processing complexity, QUAC was chosen by the fact that as a standard extension in ENVI it requires no prior information. Third, two images covered study area have been mosaic by Map Based Mosaic tool into the same coordinate (UTM, Zone 50 N, WGS-84). Colour balancing setting was complied with the standard that image with larger study area cover as the fixed image and another as adjust image and stats from overlapping regions. At last, images were resized by study area shapefile by Resize Data tool with nearest neighbour resampling method.

### **2.2.3. Samples for training and validation**

In this research, three sets of samples need to be collected for following using: the validation set for water extraction result, the training set for the land cover map, the validation set for the land cover map.

The validation sample set for water extraction result accuracy assessment have been collected by visual interpretation. Considering the resolution of Landsat TM and OLI image is sufficient to distinguish water surface and land, the visual interpretation sample has been collected based on selected Landsat image. For each image, around 200 samples have been collected. The selection of sample site based on random sampling to avoid bias, 200 points have been randomly generated in ArcMap and assigned to classes manually. The criteria of visual interpretation basically based on common sense of water surface in the true colour image, and the near infrared band have also involved in distinguishing water surface. In the sample set, both river, lake, shallow water and fishpond have been assigned to water class, a small number of sample that hard to distinguish have been deleted.

The training and validation sample set have been built for land cover classification by visual interpretation sampling. Considering in this research both land cover map and lake map in 2013 were based on the same satellite images, the lake area in the land cover map should follow the result of NDWI threshold classification result. Thus, the sample in the land cover map have been taken after the lake maps were produced, and the analysis extent of the land cover map have been masked by lake area in 2013 dry season. In the land cover map training set, samples have been taken by Region of Interest (ROI) tool in ENVI. Both images from wet and dry season in 2013 have been involved in distinguishing land cover type. In some indistinct area, images from Google Earth Pro in close years around 2013 have been used to reference (“Google Earth,” 2017). In each class around 300-500 pixels have been selected for training. The validation set has been taken in ArcMap by randomly generated 200 sample points. Then combine information from Google Earth Pro and Landsat OLI image in both dry and wet season, manually assign class for each sample by visual interpretation.

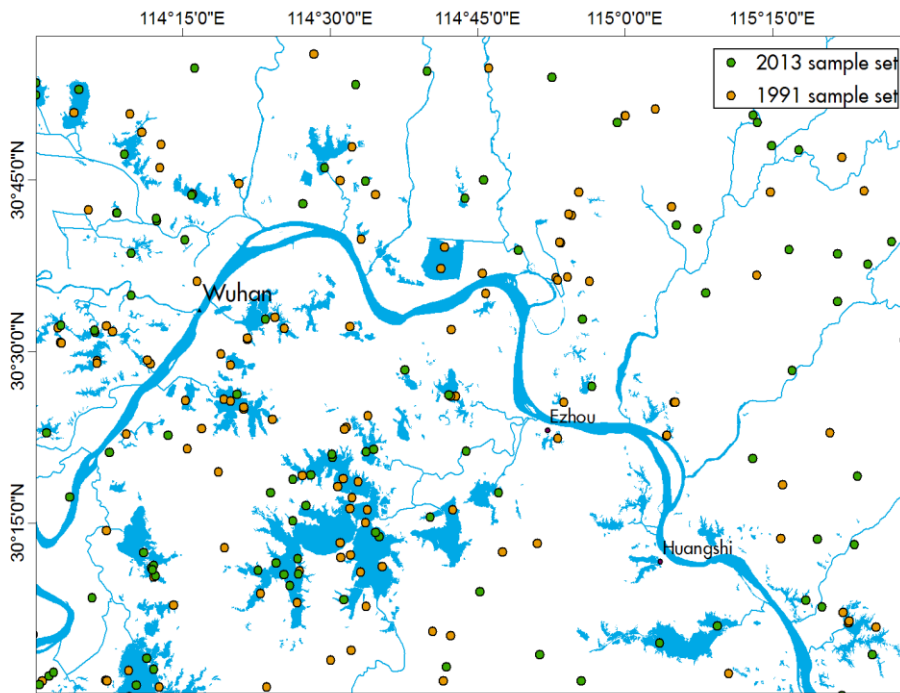


Figure 6 Sample plots of water presence and absence data used in the images in 1991(orange) and 2013(green).

Table 1 Description of data used in this study and their usage.

Data type	Acquired date	Information used	Remarks
Google Earth Online	Around 2013	Ground truth in 2013	<a href="https://www.google.com/earth/">https://www.google.com/earth/</a>
Open Street Map	Up to 2014	The Yangtze River and its branches river information	<a href="http://www.mapcruzin.com/">http://www.mapcruzin.com/</a>
Topographic map 1945	1953	Lake distribution in 1945	Topographic map
Landsat TM	19, July 2013	Lake distribution in 1991 dry season	Path=123, Row=39, 200
	28, July 2013	Lake distribution in 1991 dry season	Path=122, Row=39, 209
	30, September 2013	Lake distribution in 1991 wet season	Path=122, Row=39, 273
	7, October 2013	Lake distribution in 1991 wet season	Path=123, Row=39, 280
	24, July 2013	Lake distribution in 2013 dry season	Path=122, Row=39, 205
Landsat OLI	31, July 2013	Lake distribution in 2013 dry season	Path=123, Row=39, 212
	3, October 2013	Lake distribution in 2013 wet season	Path=123, Row=39, 276
	12, October 2013	Lake distribution in 2013 wet season	Path=122, Row=39, 285

## 2.3. Methods

### 2.3.1. Object-oriented image processing

The object-oriented classification was used to extract lake distribution information from the scanned topographic map in 1945.

As one of the legacy paper map digitise approaches, in 2009, Kerle and Leeuw have studied the object-oriented image processing technique could be an optimal solution of digitisation, which has been proved an accuracy between 94.6% and 98.5% for automatically extracted different symbol sizes on the map of Kenya in 1962. The Object-Oriented Analysis (OOA)-based processing was implemented in a Definiens Process Tree, comprised more than 50 individual routines, including repeated segmenting, merging, classification based on parameters, statistics calculation and vector export. The information extraction was carried out in Definiens software, formerly known as eCognition, allows a user-guided segmentation of an image at different scales. Some research also amid at the automatic extraction method for varieties of information on scanned maps. Levachkine, Velázquez, Alexandrov, and M (2002) carried out research on the Semantic analysis and recognition of raster-scanned colour cartographic images. Pezeshk and Tutwiler (2011) suggests the OOA-based processing technique could be able to extract information feature and text information from scanned maps.

Different with conventional pixel-based image analysis techniques, Object-oriented analysis works with homogenous image segments. Object-oriented analysis imitates the human eye and mind to evaluate the group of pixels. In the segmentation process, an image will be subdividing into more or less homogeneous units, and these units will be refined and form image objects, which representing features of interest. An object is a set of pixels that are grouped together based on user defined criteria for size, shape, texture, colour and context. Thus, an object could represent a building or a group of buildings.

### 2.3.2. 1945 lake mapping

The lake distribution in 1945 have been mapped based on the topographic map made in 1953, all the lakes larger than 5 km<sup>2</sup> on the topographic map were the objectives of this research. To extract these lakes from the scanned topographic map, the Object-oriented classification has been applied by eCognition software. With the georeferenced topographic map, a set of process have been built to extract lake vector layer.

The features used in object-oriented classification was evaluated on object level instead of conventional pixel level. Six features have been involved in this classification process tree, respectively are area of the object, average brightness of the object, maximum difference (Max.diff) which indicate the strong colour contrast in target object, border Relations to neighbour object (Rel.border) which indicate the extent of object surrounded by specific class, and two colour based custom feature designed to amplify the difference between background area and lake area. The formula of the custom features as follow:

$$\text{Feature1} = B_3 - B_1$$

$$\text{Feature2} = 2 * B_1 - B_2 - B_3$$

$B_i$  is the average band value of the object, in this image  $B_1$ ,  $B_2$  and  $B_3$  correspondent to Red, Green and Blue layer of the image, respectively.

In eCognition software, image has first been fragment into object polygons, then the geometry and spectrum feature will be calculated based on these polygons (objects). In this research, the process tree followed the idea that remove irrelevant background objects, and the remaining polygons are lakes. Two

classes have been built in this process, the background and lakes. Initially, all polygons have been assigned to lake class. The process tree executed as follow steps:

- Image segmentation: A vector layer has been built based on parameters which gives ideal separability of different objects and symbols, as well as the size of segment polygons. All the polygons have been assigned to lake class.
- Remove background elements: Lake with Brightness > 200, Feature1 between 10~90 have been assign to the background.
- Majority analysis: Isolated background (Rel. border to background=0) have been assigned back to the lake, then lake with Rel. border to background > 0.8 have been assign to the background.
- Merge connected polygons in both classes.
- Noise filter: lake with area under 100 pixels and Max. diff. < 0.3 have been assign to the background, and background with Rel. border to water and Feature2 > 22 have been assign to the lake.
- Small lakes filter: lake with area under 30 pixels and Rel. border to background = 1 have been assign to background
- Merge lake class and export as shapefile.

Although most lake areas have been well extracted into the vector layer, there still existed some misclassification, including the area in lakes affected by symbols and the symbols outside of lakes been misclassified into lakes. To solve this problem, the manually visual interpretation was performed in ArcMap software. After the object-oriented classification, the shapefile of lakes has been imported into ArcMap geodatabase and proceeded to post-processing. In post-processing, the lake area affected by symbol have been patched, and misclassified lakes have been removed manually. At last, irrelevant water areas have been removed from lake layer, including lakes under 50000 m<sup>2</sup>, the main canal of The Yangtze River and its branches.

### 2.3.3. McFeeters' Normalized Difference Water Index

In order to extract lake distribution information from Landsat satellite images, the Normalized Difference Water Index (NDWI) was involved to this research.

As one of water indices have been widely used because of high accuracy in water body detection and low-cost implementation, the Normalized Difference Water Index (NDWI) (McFeeters, 1996) is a satellite-derived index using green and near-infrared(NIR) wavelengths to monitor changes related to water content in water bodies. The McFeeters' NDWI is computed as:

$$NDWI = \frac{X_{green} - X_{nir}}{X_{green} + X_{nir}}$$

where  $X_{green}$  refers to the green band, and  $X_{nir}$  refers to the NIR band

This formulation of NDWI produces an image in which the pixels have positive value are typically open water areas, and the negative values area typically non-water features. However, in most cases, a threshold has been applied instead of positive and negative value. In other words, images could be classified as water or non-water by identifying a threshold value. In 2016, Liu, Yao, and Wang suggested that it might be better to set the McFeeters' NDWI threshold to -0.05 instead of 0 used in many cases. However, the most optimised threshold in different study area still needs to be calibrated and confirmed based on different conditions.



### 2.3.4. Landsat image lake mapping

To extract lake distribution information from Landsat satellite image, NDWI threshold classification was used for both Landsat TM images in 1991 and Landsat OLI images in 2013. In this case, NDWI threshold classification has been performed on both types of images which have close band composition in visible bands and near infrared band. Considering the difference of bandwidth and sensor type, the settings of threshold have been considered separately. The objective lakes were extracted on the basis of the lakes in 1945 extracted from topographic map.

NDWI threshold classification was performed in ENVI software. Four pre-processed images have been transformed into NDWI DN value map through band math tool, with the command formula below:

$$\text{fix}(((\text{float}(b1) - b2)/(b1 + b2)) * 10000)$$

in the formula, b1 instead of Green Band and b2 instead of Near Infrared band.

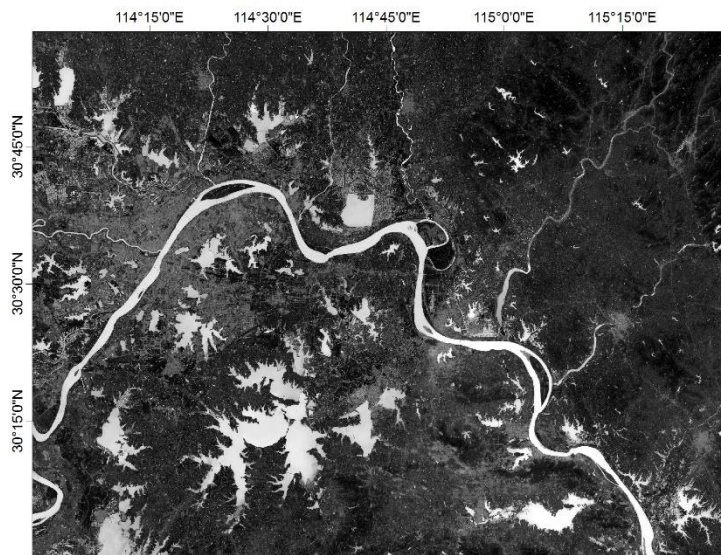


Figure 7 Calculated NDWI value image in the dry season of 2013.

In Landsat TM images, the green band is band 2, and the NIR band is band 4, respectively correspondent to b1 and b2. In Landsat OLI images, the green band is band 3, and the NIR band is band 5, respectively correspondent to b1 and b2 in the formula. For easier counting and operating, the NDWI value was multiplied by 10000.

After got the NDWI images, the proper threshold was selected for each image. According to the definition of NDWI, in the optimal situation, the threshold would be setting as 0, and all the pixel with a higher value than 0 is water, vice versa. In this research, the threshold was selected based on the best separation between lake and other landcover types. The threshold for NDWI maps generated from TM images was selected as -0.05, which gives the best separation. For NDWI maps generated from OLI images, the threshold was decided as 0.05. At last, all NDWI images was classified based on selected threshold through decision tree tool in ENVI. All the pixels with a higher value than threshold have been assign to water. Then the classified water pixels were transformed into vector layer and added into ArcMap geodatabase as polygon feature class for further post-processing.

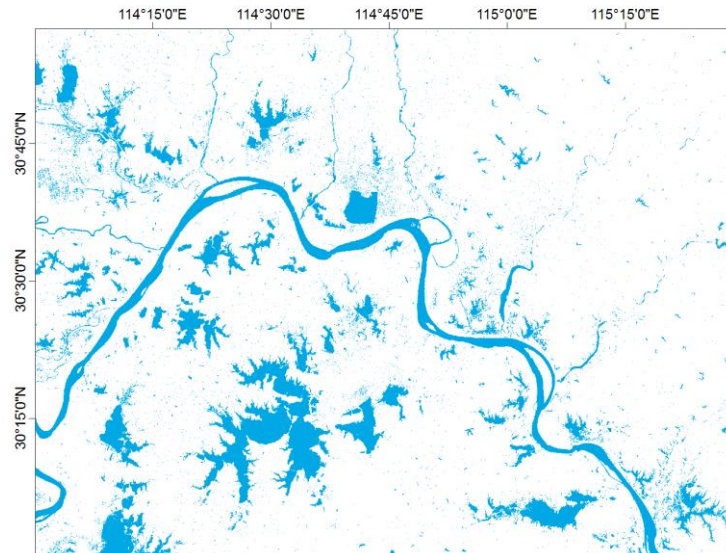


Figure 8 The threshold-based water extraction result of the NDWI image in the dry season of 2013, the threshold of this image has been set as 0.05

The post processing of polygon feature class layers performed in ArcMap software based on two criteria: patch the relevant lake polygon and remove irrelevant water surface (river, paddy field, lakes irrelevant to extracted lakes in 1945). In doing so, the following steps were performed: remove lakes smaller than 50000 m<sup>2</sup>, remove river and lakes irrelevant to extracted lakes in 1945, remove misclassified paddy field and patch the objective lakes, and give lakes new attribute about river-connection status. In the polygon feature class layers, each object basically could be considered as a lake. First, in the attribute table, all the objects smaller than 50000 m<sup>2</sup> have been removed considering the misclassified noise and small lakes. Second, based on the map of lakes in 1945, objects have no overlap with lakes in 1945 have been considered as irrelevant lakes and removed. In this step, all the rivers have been removed manually. Third, the incomplete objects and lost lakes have been patched manually by visual interpretation. At last, every object has been assigned new attribute Connection to River (CTR), through visual interpretation, the open lakes have been assigned CTR value 1 and closed lakes have been assigned CTR value 0.



Figure 9 The post-processed water extraction map of the dry season in 2013, i.e. the final lake distribution of the dry season in 2013

### 2.3.5. Support Vector Machines classifier

In this study, Support Vector Machines classification algorithm was applied to acquire the land cover information from Landsat OLI images.

Over past decades, many research have been done to exploit machine learning methods to classify remote sensing images, science neural networks (NN) have been introduced into remote sensing field. Many different models and paradigms of NN have been used for image classification; they are standard Multilayer Perceptron (MLP) network, Radial Basis Functions (RBF) neural network, structured neural networks and hybrid architectures. All these methods share as the common idea that performs the learning of the classification algorithm according to the minimization of the empirical risk. However, the newest machine learning approaches in remote sensing are build based on the idea which allows tuning the trade-off between generalisation capability and empirical risk. The structural risk minimization principle is the base of the support vector machine (SVM) classification approach. Comparing with NN approaches, SVMs have followed advantages: higher robustness to the Hughes phenomenon and higher generalisation, require less effort for the model selection in the learning phase and the implicit automatic architecture definition, optimality of the solution obtained by the learning algorithm (Fowler, 2000).

SVM is a supervised machine learning classification technique, based on statistical learning theory. By determining the location of decision boundaries, it could produce the optimal separation of the classes. This technique consists of the input and output layers, and as an important factor, proper kernel type needs to be selected for optimal classification result. This study will perform Radial Basic Function kernel as it requires the definition of a few parameters and also shown to produce a generally promising result (Rokni, Ahmad, Solaimani, & Hazini, 2015). The Gamma in kernel function controls the model complexity for fitting training data set. The penalty parameter controls the trade-off between allowed errors. And the classification probability threshold should be set to zero forcing all pixels to be classified into a class label and no pixel unclassified.

### 2.3.6. Land cover map producing

According to the research objective demand, the land cover type on filled or vanished lake area has been sorted as four classes: forest, build-up area, agricultural land, and bare soil. The build-up area including the road, residential area, and industrial area. Agricultural land including the farm, paddy field, and artificial fish pond. Water area has been treated as two types: the lake area was not involved in land cover classification, and the river area have been classified as river class. Thus, there are six classes in the final output land cover map, including five classes from land cover classification and lake area from Chapter 3.2.

Table 2 Definition of each land cover class in the land cover map 2013.

Class name	Defination
Forest	Forest area
Build-up	Urban area, including residential area and industrial area
Farm	Agricultural area, including the paddy field and normal farm
Baresoil	Bare soil
River	The yangtze river and its branches
Lake	Lake area from the image in the dry season of 2013

Images from both dry and wet season in 2013 have been involved in classification, in order to combine multi-temporal information. A new layer stack has been generated with both two images in 2013 dry and wet season.

The land cover classification was performed in ENVI software with Support Vector Machine (SVM) classification tool. Before classification, the lake area extracted in the previous chapter have been used as a mask during classification. The classification parameters have been set as follow: Radial Basis Function Kernel have been used because it provides a good classification result and uses fewer parameters. The Gamma in Kernel Function was set as the default value in ENVI as 0.071. The Penalty Parameter was set as 100 to get the most accurate possible model. Pyramid Levels was set to 0 as the image should be processed in full resolution. The Classification Probability Threshold was set as 0 to make sure every pixel has class. Collected ground truth sample ROI (Chapter 2.3) was used for training SVM classifier. At last, lake class in the output land cover map have been assigned to the masked area.

### 2.3.7. Fragmentation index

The spatial pattern and fragmentation analysis were performed on both pixel and vector level. FRAGSTATS software designed to compute a wide variety of landscape metrics for categorical map patterns (McGarigal, Cushman, & Ene, 2012), which used to calculate Landscape Shape Index (LSI) in this study. LSI indicated the degree of landscape being divided into parts, namely the complexity of the geometric shape of class. It reveals the degree of impact of human activities on the pattern changes of landscape and calculated by followed formula:

$$LSI = L/2\sqrt{\pi TA}$$

L is the total perimeter of lake landscape

The Total area of Lakes, Number of Lakes, Average Lake area and Largest Patch size were calculated in vector level. These four basic indices intend to evaluate the lake changes in coverage aspect. Total area of Lakes could be an indicator of the total lake coverage change. Number of Lakes intend to indicate the total distribution of lakes in one aspect, combining with Number of Lakes could demonstrate the geometry dispersion level of lakes. Largest Patch size used to assess the fragmentation of lakes in an

indirect aspect because large patches are rare and valuable in the fragmented habitat. Comparing the value of Number of Lakes, Average Lake area and Largest Patch size in different years could indicate the fragmentation degree of lakes.

Table 3 The statistical measurement indices used in the quantification assessment of lake changes in this study and their meanings.

Indices	Meanings
Total Area	The total area of lakes
Number	The total number of lakes
Average area of lakes	The average area of lakes
Largest Patch size	Area of the largest lake
Landscape Shape Index	An indicator of geometry complexity

### 2.3.8. Accuracy assessment

Accuracy assessments of the output maps (lake maps and land cover map) in this research was summarised using confusion matrix, also known as error matrix, in which user’s accuracy, producer’s accuracy and overall accuracy were involved in assessment. In the confusion matrix, each column indicates the instances in class prediction and each row indicate the instances of actual, vice versa. Overall accuracy is a basic index measuring the error or accuracy of classification derived from confusion matrix, which sometimes not persuasive enough. Thus, the Cohen’s Kappa coefficient was employed to assess the accuracy.

Kappa coefficient and z-value test were used to statistically compare the classification accuracies of the maps. The Cohen’s kappa statistic is a chance-corrected measure of agreement (Cohen, 1960). As one of confusion matrix derived method which could avoid the chance bias, and make use of all the information from confusion matrix. As the common choice for image classification accuracy assessment (Malahlela, 2016), Kappa coefficient ranges from 0 to 1. Landis and Koch (1977) suggested that the performance of model could be considered as excellent when Kappa > 0.75, fair to good (0.4-0.75), or poor(Kappa<0.4). In Kappa z-test (Congalton, 1991; Skidmore, 1999), a statistically significant difference at 95% confidence between two Kappa statistics suggested exist when z-value equal to or larger than 1.96, which based on a two-sided P value not greater than 0.05. Generally, the larger z-values indicate more statistically significant results.

Table 4 Confusion matrix derived measures of classification accuracy and pairwise comparability.

Measure	Formulae
Overall accuracy	$OA = \frac{\sum \text{True positive} + \sum \text{True negative}}{\sum \text{Total population}}$
Kappa	$k = \frac{p_0 - p_e}{1 - p_e}$
Kappa z-test	$Z \text{ value} = \frac{\widehat{k}_1 - \widehat{k}_2}{\widehat{\sigma}(\widehat{k}_1) - \widehat{\sigma}(\widehat{k}_2)}$

$p_0$  is observed proportionate agreement, which equals to OA, and  $p_e$  is the probability of random agreement.

### 3. RESULTS

#### 3.1. Distribution patterns of lakes in 1945

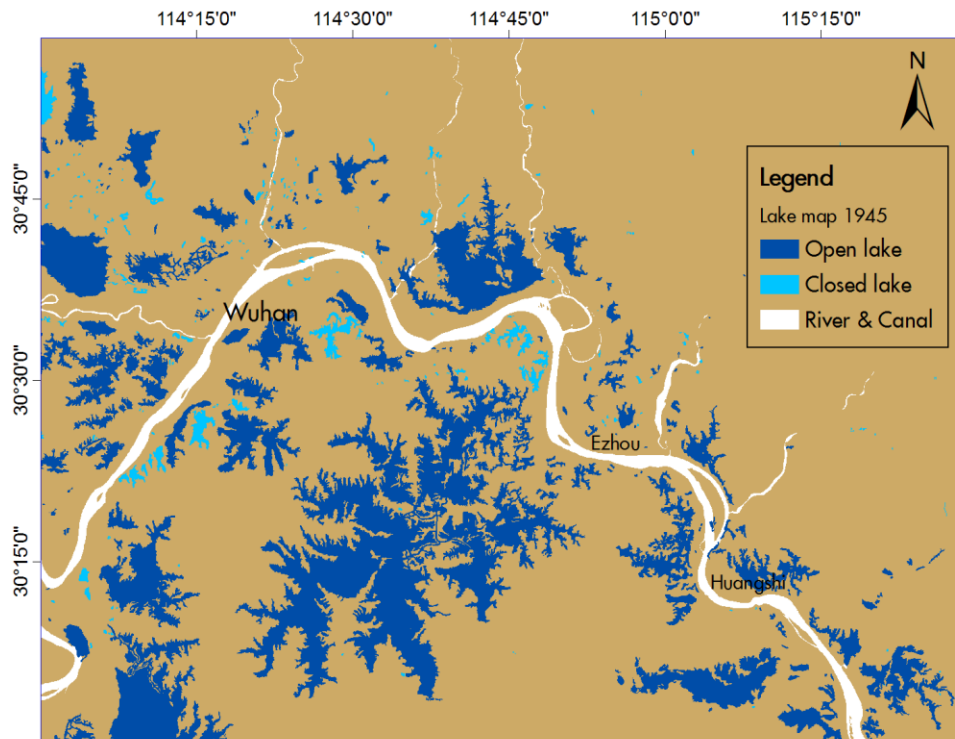


Figure 10 The open and closed lake distribution map of 1945, in which the Yangtze River have been showed only for reference.

This map showed the lake area in 1945 extracted from the scanned topographic map, in which Open (river-connected) lake and Closed (not river-connected) lake interpretation based on given streamline information on the map. All the lakes larger than 5 km<sup>2</sup> have been recorded, and the river shape is generalised polygon for reference only.

### 3.2. Distribution patterns of lakes in 1991 and 2013

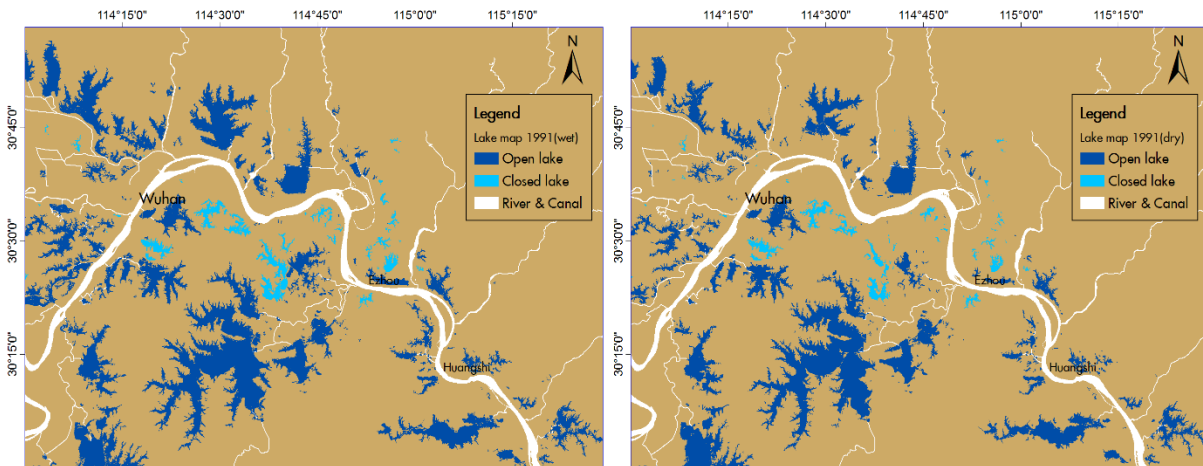


Figure 11 The open and closed lake distribution map in 1991 wet season(left) and dry season(right), in which the Yangtze River and its branches have been showed only for reference.

The lake distribution maps in 1991 have been showed above, with open and closed lakes showed in different colour. The white part on maps is the Yangtze River and its branches, used to distinguish the river connectivity of lakes. In the dry season, lakes in northwest of the map have conspicuous decrease comparing with wet season.

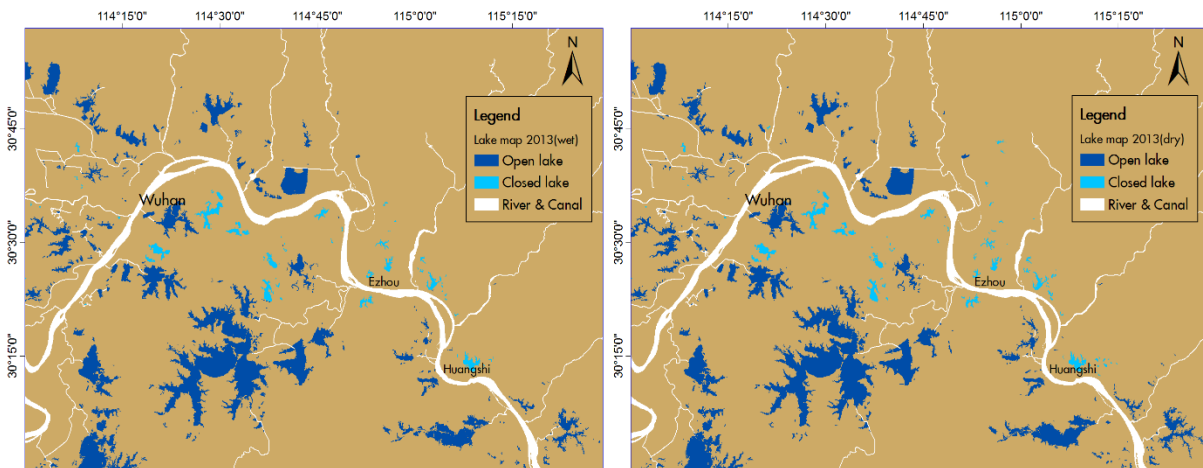


Figure 12 The open and closed lake distribution map in 2013 wet season(left) and dry season(right), in which the Yangtze River and its branches have been showed only for reference.

The lake distribution maps in 2013 have been showed above. The lake area has remarkable decrease comparing with the maps in 1991, both happened on open and closed lakes. Comparing with 1991, there is not significant change on the river connectivity of lakes in 2013. Meanwhile, the seasonal difference in 2013 is insignificant.

### 3.3. Change patterns of lakes over the last 70 years

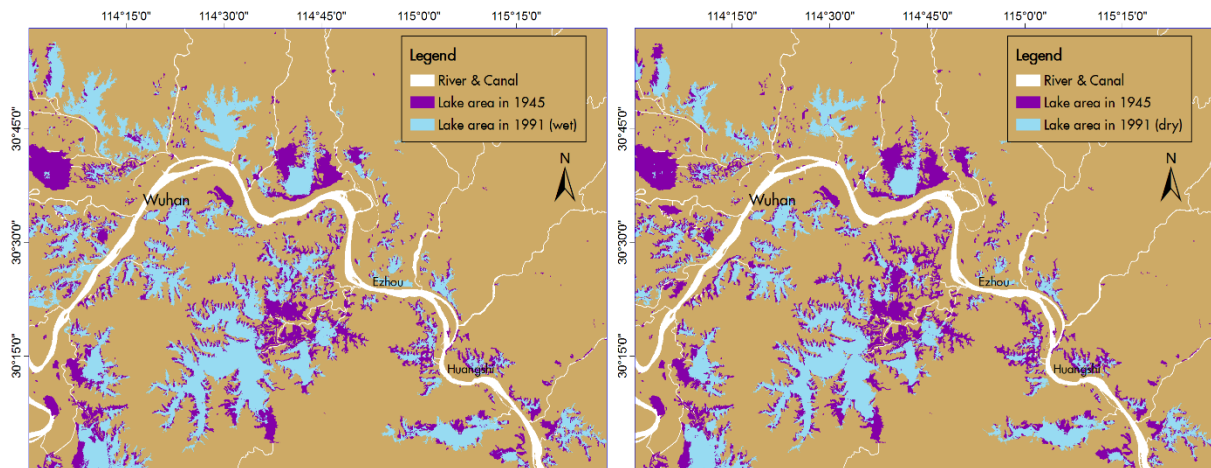


Figure 13 The lake change map between 1945 and 1991 wet season (left) and dry season(right). The purple area on the maps could be considered as the vanished lake area.

These two maps were produced to show the changes of lake extent during 1945 to 1991, remaining lakes in 1945 have been showed as blue colour, and area with dark purple colour is the former lake area in 1945. The main stream of The Yangtze River has been generalised as white polygon, and the branch streams have been indicated by white line. The river information has been extracted from 2013 satellite image and Open Street Map online database, only for reference.

Comparing two maps extracted from dry and wet season in 1991, distinct lake extent difference could be overserved, which in wet season some lake significantly larger than in dry season. Considering the historical record, this difference mainly caused by the catastrophic flood happened in 1991 along the Huai river. However, the distinct lake area decrease could be observed in these maps.

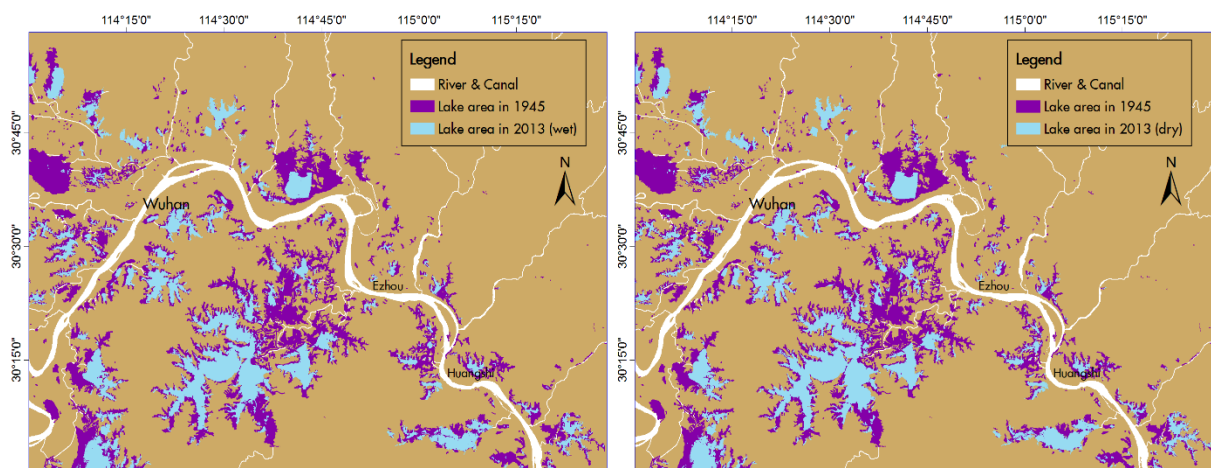


Figure 14 The lake change map between 1945 and 2013 wet season (left) and dry season(right). The purple area on the maps could be considered as the vanished lake area.



These two maps were produced to show the changes of lake extent during 1945 to 2013, lakes existed in 2013 have been showed as blue colour, and lakes area in 1945 have been showed as purple colour. The Yangtze River and branches have been showed as white colour.

There is no significant difference between lake areas in two seasons. However, it should be noted that there is rarely few lake area in wet season have been covered by lotus canopy, which affected the lake extraction. Most effects have been corrected by manually visual interpretation, but some still remaining.

**3.3.1. Statistic Result**

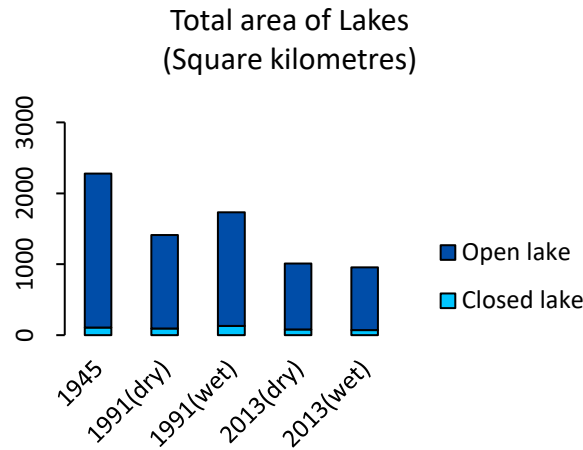


Figure 15 Bar plot of the total area of lakes calculated from five lake distribution maps, with open and closed lakes separately.

The total area of lakes in 1945 is 2279 km<sup>2</sup>, and up to 1991, the total area of lakes decreased to 1410 km<sup>2</sup> in dry season and 1731 km<sup>2</sup> in wet season, which decreased 24% to 38% comparing the total lake area in dry and wet season respectively. In 2013, the total area of lakes kept decreased to 1008 km<sup>2</sup> in dry season and 967 km<sup>2</sup> in wet season. on the basis of lake area in 1945, the area in 2013 has decreased 56% to 58% comparing the total lake area in dry and wet season respectively.

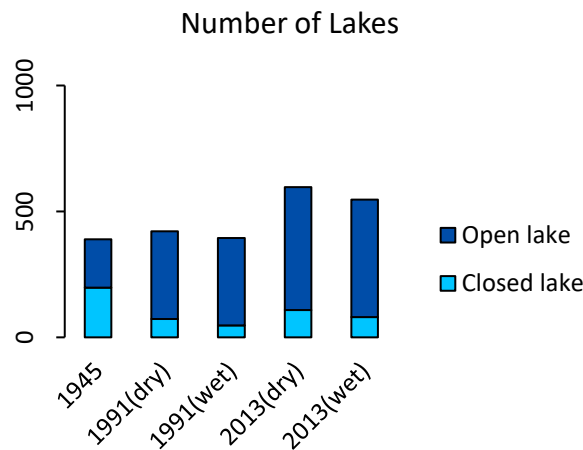


Figure 16 Bar plot of the number of lakes calculated from five lake distribution maps, with open and closed lakes separately.

The total number of lakes in 1945 is 389, with 192 open lakes and 197 closed lakes. Up to 1991, the total number of lakes slightly changed to 395 in wet season and 421 in dry season, in which the number of closed lakes significantly decreased, and the number of open lakes increased. Until 2013, the total number of lakes raised to 547-596 in wet and dry season respectively, and the ratio of closed lakes remain a small portion in total lakes.

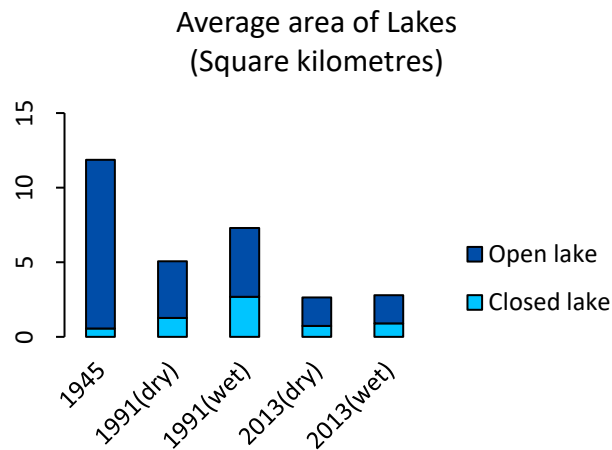


Figure 17 Bar plot of the total area of lakes calculated from five lake distribution maps, with open and closed lakes separately.

The average area of lakes in 1945 is 5.86 km<sup>2</sup>, in which the average area of open lakes and closed lakes are 11.30 km<sup>2</sup> and 0.55 km<sup>2</sup> respectively. In 1991 dry season, the average area of lakes decreased to 3.35 km<sup>2</sup>, with open lakes and closed lakes are 3.79 km<sup>2</sup> and 1.27 km<sup>2</sup> respectively. In 1991 wet season, the average area of lakes is 4.38 km<sup>2</sup>, with open lakes and closed lakes are 4.62 km<sup>2</sup> and 2.69 km<sup>2</sup> respectively.

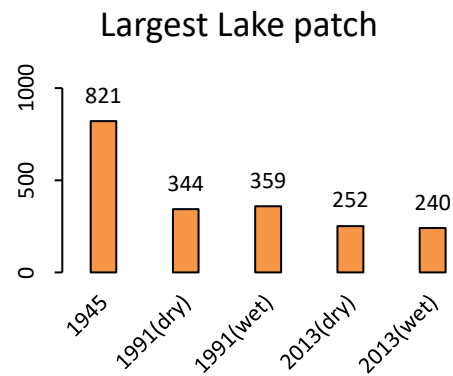


Figure 18 Bar plot of the largest lake patch size calculated from five lake distribution maps.

The largest lake patch in 1945 is 821 km<sup>2</sup>, which decreased to 343 km<sup>2</sup> to 359 km<sup>2</sup> in 1991 dry and wet season respectively. In 2013, this number kept decreased to 240 km<sup>2</sup> in wet season and 252 km<sup>2</sup> in dry season.

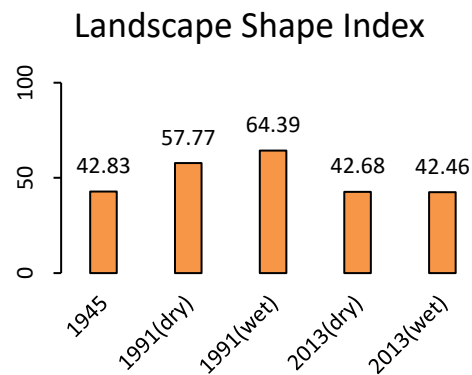


Figure 19 Bar plot of the LSI calculated from five lake distribution maps.

As one innovated wetland evaluation index, Landscape Shape Index represents the complexity of the geometric shape of the lakes. As it shown in the figure, LSI slightly raised from 43 to 58-64 during 1945-1991, then decline back to 42-43 in 2013. Although the raising number and decreasing area of lakes showed the fragmentation of lakes, LSI of lakes generally appeared a stable trend.

Table 5 The landscape attribute of lakes in 1945, the dry season and wet season in 1991 and the dry season and wet season in 2013, and the decrease percentage from 1945 and 1991 in the last two rows

Statistics Factors	1945	1991 Dry Season	1991 Wet Season	2013 Dry Season	2013 Wet Season
Number of lakes	389	421	395	596	547
Open lakes	192	348	347	488	466
Closed lakes	197	73	48	108	81
Total length (km)	8045.50	8646.76	10660.47	5386.64	5212.12
Total area (km <sup>2</sup> )	2279.59	1410.11	1731.30	1008.12	956.55
Open lakes	2170.32	1317.44	1602.22	928.96	883.08
Closed lakes	109.27	92.67	129.09	79.16	73.47
Average lake area	5.86	3.35	4.38	1.69	1.75
Landscape Shape Index	168.51	230.26	256.21	169.65	168.52
Largest Patch size	821.25	343.79	359.01	252.06	240.21
Decrease percentage (science 1945)	-	38%	24%	56%	58%
Decrease percentage (science 1991)	-	-	-	29%	45%

The decrease percentage has been calculated by  $\text{Decrease percentage} = (\text{Total area of former year} - \text{Total area of presence year}) / \text{Total area of former year}$ , of which Total area of former year stands for 1945 and 1991 in last two rows respectively. Total area of presence year stands for the time period showed in the column header.

The statistic result showed in 1945, the number of lakes was 389 with total area 2279 km<sup>2</sup>, including 192 open lakes hold 2170 km<sup>2</sup> and 197 closed lakes hold 109 km<sup>2</sup>. The average lake area was 5.86 km<sup>2</sup>. Up to 1991, the number of lakes raised to 395-421 with total area 1410-1731 km<sup>2</sup>, including 347-348 open lakes holds 1410-1731 km<sup>2</sup> and 48-73 closed lakes hold 93-129 km<sup>2</sup>. Average lake area decreased to 3.35-4.38 km<sup>2</sup>, and the total lake area decreased 24.05%-38.14%. At 2013, the number of lakes raised to 547-596 with total area 957-1008 km<sup>2</sup>, including 466-488 open lakes holds 883-928 km<sup>2</sup> and 81-108 closed lakes hold 73-79 km<sup>2</sup>. Comparing with the map in 1945, the average lake area in 2013 decreased to 1.75-1.96 km<sup>2</sup>, and the total lake area decreased 55.78%-58.04%.

### 3.3.2. Accuracy assessment

Kappa value and Overall Accuracy (OA) was used to evaluate the accuracy of NDWI threshold water extraction accuracy for every map. The results showed Kappa values of total four map were in the range of 0.95-0.97. OA percentage in all four maps were higher than 98%. The Kappa Z-test have been calculated to evaluate the comparability between four maps (Skidmore, 1999), the result showed the pairwise Z value in the range between -1.96 and 1.96, which was not statistically significant.

Table 6 The confusion matrix of the image classified by NDWI threshold in 1991 wet season presented by the number of pixels, with overall accuracy, estimate accuracy and Kappa coefficient in the last two rows.

1991 Wet Season	Non-Water (Predicted)	Water (Predicted)	Total
Non-Water (Actual)	146	1	145
Water (Actual)	2	42	45
Total	148	43	190
Overall Accuracy	98.95%		
Kappa	0.97		

Table 7 The confusion matrix of the image classified by NDWI threshold in 1991 dry season presented by the number of pixels, with overall accuracy, estimate accuracy and Kappa coefficient in the last two rows.

1991 Dry Season	Non-Water (Predicted)	Water (Predicted)	Total
Non-Water (Actual)	163	0	163
Water (Actual)	2	31	33
Total	165	31	196
Overall Accuracy	98.98%		
Kappa	0.96		

Table 8 The confusion matrix of the image classified by NDWI threshold in 2013 wet season presented by the number of pixels, with overall accuracy, estimate accuracy and Kappa coefficient in the last two rows.

2013 Wet Season	Non-Water (Predicted)	Water (Predicted)	Total
Non-Water (Actual)	146	1	149
Water (Actual)	2	41	41
Total	148	42	190
Overall Accuracy	98.42%		
Kappa	0.95		

Table 9 The confusion matrix of the image classified by NDWI threshold in 2013 dry season presented by the number of pixels, with overall accuracy, estimate accuracy and Kappa coefficient in the last two rows.

2013 Dry Season	Non-Water (Predicted)	Water (Predicted)	Total
Non-Water (Actual)	160	0	160
Water (Actual)	2	31	33
Total	162	31	193
Overall Accuracy	98.96%		
Kappa	0.96		

Table 10 The z-statistic comparing the confusion matrix of the four images classified by NDWI threshold.

Kappa z-test	1991 Dry Season	1991 Wet Season	2013 Dry Season
1991 Wet Season	0.636753887		
2013 Dry Season	0.011112694	0.623109683	
2013 Wet Season	0.705187033	0.063785673	0.691189408

The z-statistic calculated in this table indicated the statistically significant between the confusion matrix resulted accuracy and kappa coefficient of images pairwise. Science the z-value in the range between -1.96 and 1.96, the accuracy of images suggested in a comparable range. Namely, the change detection will not be affected by the variation of accuracy.

### 3.4. Driving factors of lake changes

In the land cover map 2013, the study area has been classified into six classes, including lake area, forest cover, build-up area, agricultural area, bare soil and river.

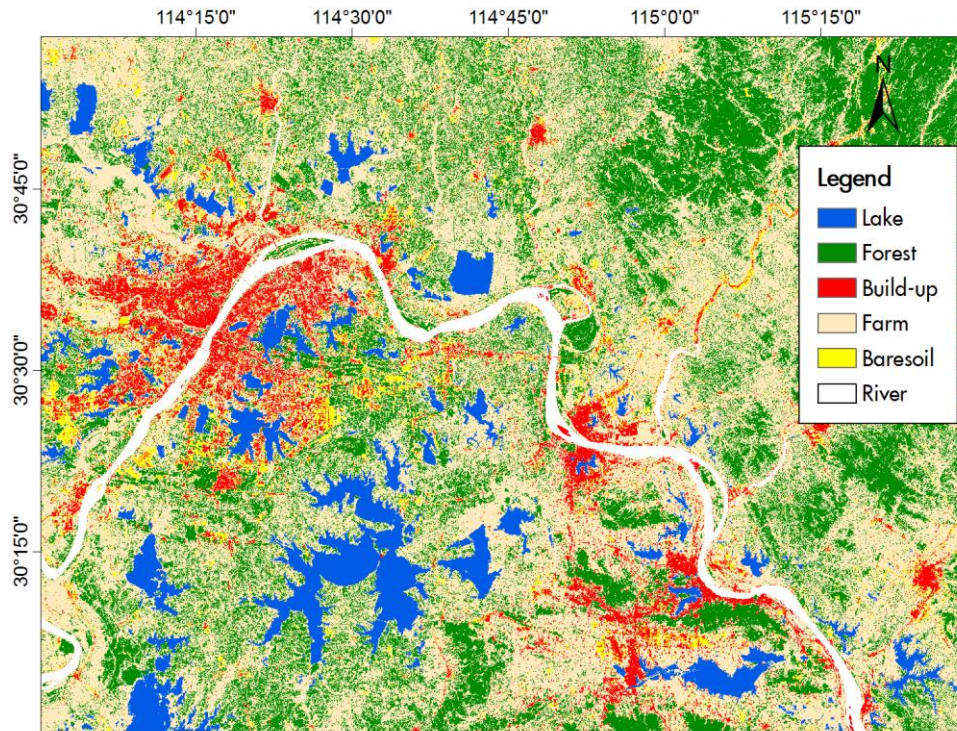


Figure 20 The land cover map in 2013.

As showed above, four major cities in the study area could be distinguished as large build-up area clusters, and bare soil occurred mostly around Wuhan and Huangshi cities. The dominant land cover class in study area is farm, which also surrounds lakes. Most forest occurred at the north-west part of the study area.

This map provides a generally land cover situation of study area in 2013. But the mainly use of this map is analysing the land cover type in the extent that lake decreased during 1945-1991 and 1945-2013. Based on this land cover map, four maps have been generated by clipping this map with lake diminished extent.

Through masking irrelevant extent, the land cover on former lake area has been highlighted. As showed above, dominant land cover on maps is farm area. Build-up area could be found mostly around major cities in the study area. A small portion of forest area could be found mixed with farm area. Four images respectively corresponding to the wet and dry season in both 1991 and 2013 have been showed below:

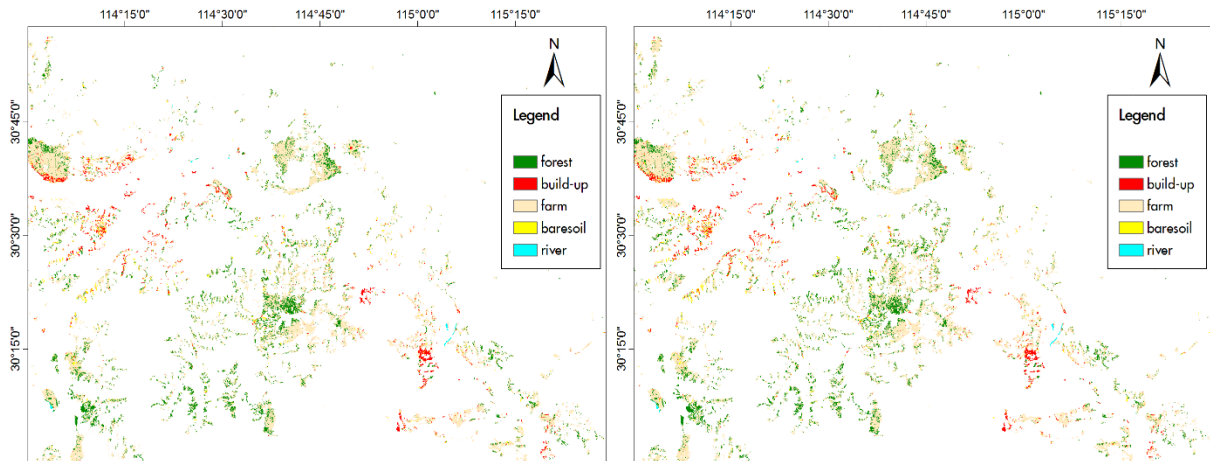


Figure 21 The partial land cover map in which the lake vanished area from 1945 to 1991 wet season(left) and dry season(right)

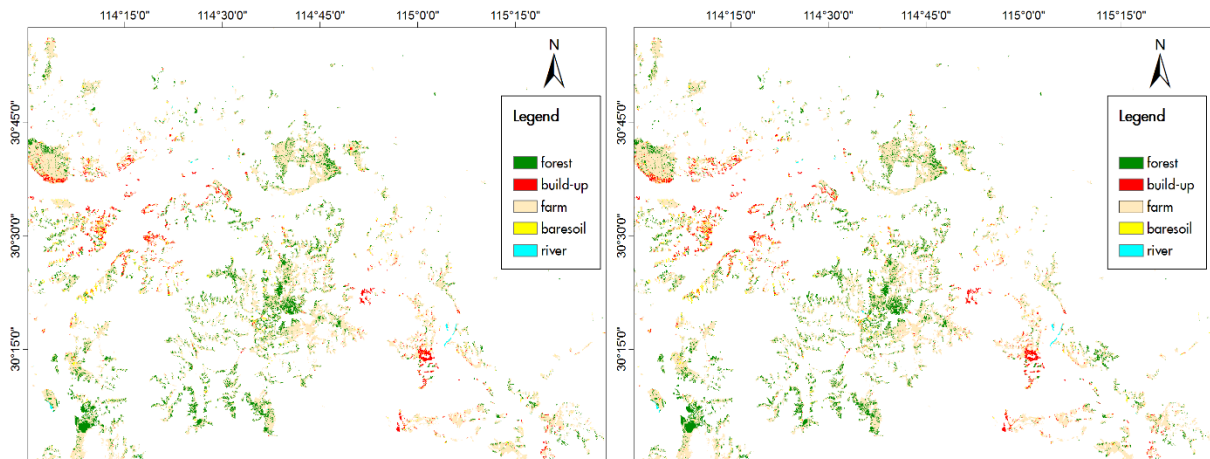


Figure 22 The partial land cover map in which the lake vanished area from 1945 to 2013 wet season(left) and dry season(right)



**3.4.1. Statistic Result**

Table 11 The occupation area and rate of five classes on the former lakes area retrieved by lake change map between 1945 and the dry season in 1991, the wet season in 1991, the dry season in 2013, the wet season in 2013 respectively.

Class	1991 wet season		1991 dry season		2013 wet season		2013 dry season	
	Area (km <sup>2</sup> )	Percentage	Area (km <sup>2</sup> )	Percentage	Area (km <sup>2</sup> )	Percentage	Area (km <sup>2</sup> )	Percentage
Farm	37423	68.25%	60290	69.34%	93535	70.70%	90169	70.92%
Forest	11551	21.07%	17772	20.44%	26518	20.04%	25188	19.81%
Build-up	3639	6.64%	5512	6.34%	7783	5.88%	7369	5.80%
Bare soil	2057	3.75%	3149	3.62%	4180	3.16%	4019	3.16%
River	158	0.29%	225	0.26%	288	0.22%	402	0.32%
Total area	54829		86948		132304		127147	

This table showed the area and percentage of five classes occupied the lakes in the classified land cover map in 2013. Namely, the numbers represent the area and percentage of certain land cover class replaced the former lakes. the land cover information is acquired from land cover map 2013 and the lake change information is acquired from lake change map 1945-1991(wet), 1945-1991(dry), 1945-2013(wet), 1945-2013(dry) respectively.

According to the statistic result showed above, lake area decreased 548-869 km<sup>2</sup> during 1945 to 1991, and the decreased area became 1271-1323 km<sup>2</sup> during 1945 to 2013. Based on produced land cover map in 2013, 69.34%-70.92% of decreased area during 1945 to 1991 is Farm class, 19.81%-20.44% is Forest class, and 5.80%-6.34% is Build-up class. 68.25%-70.70% of decreased area during 1945 to 2013 is Farm class, 20.04%-21.07% is Forest class, and 5.88%-6.64% is Build-up class. The pie-chart as follows:

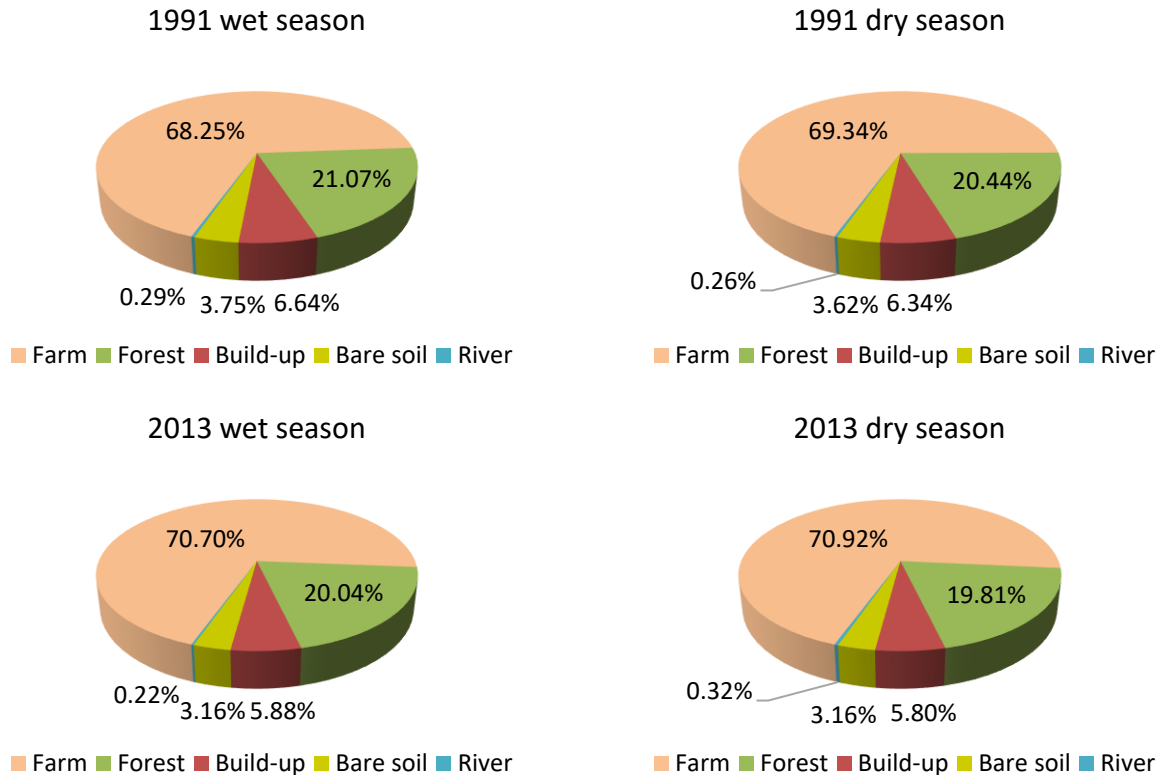


Figure 23 The pie chart of the occupation rate of each class in each image from Figure 21 and 22.

### 3.4.2. Accuracy assessment

Accuracy assessment of land cover map was using the land cover ground truth validation set (Chapter 2.2.3). Confusion matrix was generated through Confusion Matrix Using Ground Truth ROIs tool.

Table 12 The confusion matrix presented by the number of pixels of each class in the land cover map in 2013 with overall accuracy and Kappa coefficient in the last two rows.

Class	Predicted				
	River	Forest	Farm	Build-up	Bare soil
River (Actual)	6	0	0	0	0
Forest (Actual)	0	37	21	0	0
Farm (Actual)	0	4	85	5	0
Build-up (Actual)	0	0	0	34	0
Bare soil (Actual)	0	0	2	1	3
Total	6	41	108	40	3
Overall Accuracy	83.33%				
Kappa	0.74				

Table 13 The producer's accuracy and user's accuracy of each class in the land cover map in 2013, with both the percentage of accuracy and proportion of pixels

Class	Prod.Acc. (Percent)	UserAcc. (Percent)	Prod.Acc. (Pixels)	UserAcc. (Pixels)
River	100	100	6/6	6/6
Forest	90.24	63.79	37/41	37/58
Farm	78.7	90.43	85/108	85/94
Build-up	85	100	34/40	34/34
Bare soil	100	50	3/3	3/6

The Prod.Acc is the abbreviation of producer's accuracy and the UserAcc. is the abbreviation of user's accuracy, both measure have been showed as sample pixels and its percentage, of which producer's accuracy indicates the accuracy of classification, user's accuracy indicates the reliability of classes in the classified image (Congalton, 1991).

The accuracy assessment of land cover classification map was assessed by OA and Kappa value. The result showed the Kappa value is 0.74, and the OA is 83.33%. In the confusion matrix both Product Accuracy (PA) and User Accuracy (UA) of River class is 100%, in Forest class PA is 90.24 and UA is 63.79, in Farm class PA is 78.7%, and UA is 90.43%, in Build-up class PA is 85% and UA is 100%, in Bare soil class PA is 100%, and UA is 50%.



## 4. DISCUSSION

### 4.1. Lake changes in the middle reaches of the Yangtze River over the last 70 years

#### 4.1.1. Detecting and quantifying lake changes

The result showed a significant decrease in the total area of lakes, which correspond to the result of previous studies and relevant literatures. Meanwhile, the number of lakes appeared stable during 1945-1991 and increased between 1991 and 2013. This change led to further decrease of the average area of lakes, which decreased at the same rate as the total area of lakes during 1945-1991, and after 1991, the average area of lakes decreased sharply with the rising number of lakes. Generally, it showed the total area of lakes keep decreasing during 1945 to 2013, and a remarkable fragmentation happened after 1991.

In 2010, xu et al. have studied the wetland changes in Wuhan urban area, and the result showed lake wetlands decreased 18.71% from 1987 to 2005. The corresponding result has been showed in this study: during 1991 to 2013, the total area of lakes in study area decreased about 29%-45%. Similar study faced on larger area along The Yangtze River also suggest corresponding trend of lake changes during this period. Cui et. al have studied the lake in the middle and lower reaches of the Yangtze River basin, which showed in Hubei province, the lakes area decreased 1289 km<sup>2</sup> during 1990 to 2000, and continue decreased 203 km<sup>2</sup> during 2000 to 2008. However, according to the study by Cui et al. in 2013, the lake area in Hubei province decreased 801 km<sup>2</sup> during 1950-1970, then increased 850 km<sup>2</sup> during 1970 to 1990, which generally no significant change during 1950-1990. This result to conflict with the result in this study, which showed the total area of lakes decreased 24.05% to 38.14%. The further study still needs to be carried out to explain the lake change difference between the study area and Hubei province.

#### 4.1.2. Flood and non-flood seasons

The lake information in 1991 and 2013 have been acquired from dry and wet season intend to have possibly convincing change detection when comparing with lake distribution in 1945. The result showed a significant total area difference in 1991 wet and dry season, in which the total area of lakes in wet season have 321 km<sup>2</sup> more than in dry season, which means 22.78% of total area of lakes in dry season. However, in 2013, the total area of lakes in dry season have 52 km<sup>2</sup> (5.39%) more than in wet season. Factors caused this phenomenon have been discussed in follow paragraph.

According to relevant researches, multiple factors involved causing this happening: the perception variation, influence from new built lotus pond, the filling of lakes. According to research conducted by Cui et al. (2013), the water level of lakes along the Yangtze River exists huge difference between different seasons. At the same time, during the early 1990s there was several catastrophic floods happened in the middle reaches of The Yangtze River, which could be one of the reason caused the huge difference of lake area between wet and dry season in 1991. The filling lakes also considered possibly one of the causes, because through the filling lake activities during 1991 to 2013, most seasonal shallow lakes could be filled. The last factor involved is the lotus pond built during 1991 to 2013. In the research conducted by Wang et al. in 2008 the lotus pond has been sorted as one of the major artificial wetland landscape which growing rapidly science 2000s. However, due to the canopy cover above water surface in summer season, the lotus pond is hard to be distinguished by satellite image. The total lake area in wet season of 2013 is slightly less than dry season possibly caused by the lotus ponds.

## **4.2. Driving factor of the lake changes**

As the result shown, the dominant land cover class of which replaced former lakes is farm area, which occupied over 70% of the total. Subsequently is forest, takes up 20% of the total. Build-up area only takes about 6%. It turns out the driving factor of lake degradation in large extent cannot be represented by the urban expansion. In the study area, the driving factor more tends to be agricultural land expansion.

Literature records suggested multiple factors involved the lake changes over past 70 years in different extent along the middle reaches of The Yangtze River. Studies by Xu et al. (2010) and Wang et al. (2008) indicates the urban expansion is one important factor leading to the lake shrinking, Cui et al. (2013) also studies the historical policy impact on lakes in a larger extent covered middle and lower reaches of The Yangtze River. This study constructed based on evidence in the previous study, namely, the main driving force of lake decrease is human activity. In this study, a different method was used to evaluate the demand of land behind the change of lakes in the middle reaches of The Yangtze River. Through highlighting the land cover map by the former lake area, it is able to see the land cover types on these former lakes. Further, it could explain the driving factor in certain level.

Focused on the change of lakes happened in Wuhan city over past century, many studies had been carried out. The rapid economic development and the population explosion have been always considered as the fundamental reason caused the sharp decrease of lakes in Wuhan city, specific including lake filling and artificial enclosure, which have been generally recognized as the driving factor of lake decrease. Similar research focused on large extent covering Hunan, Jiangxi, Hubei, southern Anhui, and southern Jiangsu provinces, and Shanghai municipality have been carried out by Cui et al. (2013), which covered 130 years with relevant evidence collected from varieties studies carried on their study area. According to their field surveys and previous literature, factors caused the change of lakes in the middle and lower reaches of the Yangtze River was sorted as human activities and natural events. However, human activities including lake reclamation, and expansion of lakeside developments and enclosures attributed more than natural events (e.g., climate change, flooding, soil erosion, and sedimentation). During 1950 to 1970, the reclamation of land-surrounding lakes happened at an unprecedented rate. However, the reclamation also caused the change of lakes' shape which led to the increase of lake area, and at the same time, the establishment of dams could also cause the expansion of lakes in some extent. During 1970 – 1990, the demands for fish rearing resulted some lakes were converted into aquaculture ponds. Long-term lake reclamation caused the increased sedimentation accumulation and the raise of lake bed level, which affected the water capability of lakes. Consequently, during several catastrophic floods in late 1980s and early 1990s, the lake area had an increased trend. During 1990-2008, due to the reclamation or expansion of lakeside development and enclosures, the lake area decreased again.

## **4.3. Mapping the lake change maps and land cover maps**

### **4.3.1. The use of scanned legacy maps**

In recent decades, with the benefit of satellite images and remote sensing technics, the acquisition of geographic information became accessible than way past. However, the first satellite was launched in 1957, and existing legacy maps is the only way to obtain geographic information prior to this date. Thus, the extraction and utilisation of information in these legacy maps appears to be particularly important. Kerle & Leeuw (2009) have proved the feasibility to apply object-oriented image processing techniques on legacy map information extraction. In this study, the extraction of lake distribution information from the scanned topographic map, which is the foundation of the entire research, was executed through Object-oriented classification. Although the process tree designed in this research is very simple and some symbol covered areas still need manual modification. The result turns out that Object-oriented classification have

advantages on information extraction than conventional pixel-based methods. This object-based approach could easily avoid the most noise on the scanned map, and the texture, position or shape of objects could be involved in classification.

Information from the past legacy maps is valuable, but it has to be admitted that the accuracy and precision of these maps have been limited by technique capability. Thus, how does the information from legacy maps have been used influences the reliability of the research result. In this study, the legacy topographic map of Hankou was compiled from the best available large scale map of china and partially revised by aerial photo. Since the revised area only covers half of the total map extent, some lakes in the poor-quality area could possibly been ignored. At the same time, the detailed produce criteria are not available, for instance, the minimum area of lakes have been cited is unknown. Based on the situation above, two criterions have been carried out to avoid the asymmetry of information between legacy map and classified satellite image:

- Due to the precision difference between aerial photo revised area and other area, the change detection only focused on the lakes exists in topographic map. That is, only the lakes coverage has been extracted from legacy map in 1945 would appears to be lake in the produced lake map 1991, 2013, respectively. It has to be admitted that through this procedure some increased new lakes after 1945 will be ignored. However, the objective of this research is to quantify the lake changes in study area over last 70 years, which means the same criteria of lake extraction between two period is more important than mapping as more lakes as it could be. In addition, according to historical record, the overall trend of lakes in study area is sharply decrease, in contrast the few increased new lakes could be ignored.
- Another criterion has been carried out is the minimum area of lakes have been mapped is 0.05 km<sup>2</sup>, which means 56 pixels in Landsat images and 69 pixels in the scanned topographic map. This minimum area could avoid most noise on both the classified Landsat images and the classified topographic map, and the most lake distribution information has been guaranteed.

#### **4.3.2. NDWI threshold water extraction method**

Several water extraction methods have been tested on both Landsat OLI and TM images. The result showed Simple Water Index (SWI) works well on OLI images, but when applying on TM images, result appeared not correct, in which the water area become negative value. It possible due to the difference of band width between TM and OLI images. Support Vector Machine (SVM) classification have also been tested to be water extraction method, but as a supervised classification method, it is difficult to ensure the training sample would be selected on the same standard. Thus, the comparability between images could not been guaranteed. As a conventional water extraction method, NDWI threshold approach is feasible on different sensor band width. In this research, NDWI thresholds have been selected for TM and OLI images based on the visual measure of best classification result. However, two weak point of NDWI method been noticed during research. First, the river area could not be well extracted from image in 1991 dry season, possibly due to the high volume of sediment in the river. Since objective of this research is lakes, the river could be considered as irrelevant. Second, the total area of lakes in 2013 dry season is higher than wet season have been noticed. After the visual interpretation check, certain amount of water area with lotus covered above the water surface has been found not corrected classified. This could be considered as one reason caused abnormal result between dry and wet season.

#### **4.3.3. Open lakes and closed lakes**

The river connectivity of lakes in 1945 was manually distinguished with the scanned map. Branches of The Yangtze River have been well presented in line on the map. In the criteria of determine river connected

lakes, the lake directly connected to The Yangtze River and its branches have been sorted as open lake, and the independent lake or lake indirectly connected to open lakes is considered not connected to river, namely closed lake. In the map of 2013, the river connectivity was distinguished by combining the Landsat OLI image, Google Earth Pro and Open Street Map data, using same criteria as above. Concerning the data availability in 1991, the river connectivity information was initially referred to information in 2013, namely, define the overlapped lake between 1991 and 2013 as same river connectivity. Then, through visual interpretation on Landsat TM image in 1991 to do the secondary correction.

Taking about 95% of the lake area, the change happened mostly on open lakes. Up to 1991, the total area of closed lake showed little difference with it in 1945. Between 1991 and 2013, the total area of closed lakes decreased as the same rate of the overall situation. However, the number of closed lake have changed significantly, which decreased more than a half during 1945-1991. Considering the area of closed lakes is relatively small, this situation may be caused by the different data source and criteria of two maps. Yet the change of closed lakes between 1991 and 2013 is comparable with nearly data source and same extraction criteria. The result of closed lake changes corresponding to the overall situation, which showed increased number and decreased total area, resulting in a fragmentation and decrease in area.

#### **4.3.4. Classification of land cover map**

Five classes have been arranged in the land cover map. They are forest, farm, build-up area, bare soil and river respectively. In the chosen of classes, both the resolution of satellite image and the information requirement has to be taken into consideration. The residential and industrial area is easy to distinguish and have same spectrum trait, being sorted as build-up area. Paddy field and agricultural land have been sort as farm area. Farm area have its own temporal trait, in wet season, paddy field appear similar characteristic as water surface and agricultural land appear similar like forest, and in dry season, most plant have been harvested and there become less water in the field, most appeared as bare soil. Thus, both image from dry and wet season have been used as input of classification. In the 30 meters' resolution satellite image, forest have similar spectrum trait as agricultural land, but still distinguishable in Google Earth image. In driving factor analysis, forest and farm area point to different driving factor, for this reason forest need to be classified as an independent class. At last, the information of lake area has been extracted through NDWI threshold method, and it have been used in land cover map to avoid conflict. The produce of land cover map classification has been masked by the extracted lake area, the lake area was choosing from 2013 dry season to avoid the affection of plant above water surface, and also the affection of paddy field. Although the river class is not necessary, but there still need a class contain water area, mainly from river. Final land cover map contains six classes, including five classes from land cover classification and lake area from lake extraction.

## 5. CONCLUSION AND RECOMMENDATION

### 5.1. Conclusions

This study fulfils the detection and quantification of lake changes in the middle reaches of The Yangtze River over past 70 years through techniques of remote sensing and geographic information system. The change detection based on information from topographic map in 1945 could not adequate to represent all the lakes in the study area, while the analysis based on the lakes showed in the topographic could tell the changes of these lakes over past 70 years, which is able to represent the major trend of lake variation. The land cover map in 2013, reveals the driving factor of lake changes in an innovated way comparing with previous studies. In this study, four aspects have been explored corresponding to the research hypotheses: a) change detection between lakes extracted from topographic map and lakes extracted from Landsat images in both wet and dry season. b) the seasonal difference between wet and dry season in 1991 and 2013 respectively. c) the river connectivity of lakes and its changes. d) driving factor analysis through analyse current land cover types on former lake area.

- Over past 70 years, the total area of lakes in study area appeared a rapidly decrease trend, in which more than half of lake area vanished. Specifically, total lake area lost one-third during 1945-1991, and keep decreased in higher speed during 1991-2013. The number of lakes, average lake area and largest patch size showed a fragmented trend on lake distribution. However, through the Landscape shape index analysis, the complexity of lakes remained a stable trend.
- In 1991, the lake map in wet season appeared significant difference comparing with dry season. The reason should be owing to the catastrophic flood happened in the early 1990s in the middle reaches of the Yangtze River and resulted water level increase. On the contrary, in 2013 the total lake area in wet season is lower than in dry season. This phenomenon partly because of the influence from new appeared lotus pond science 2000s, and the disappear of seasonal lakes also considered being one of the causes.
- As the result shown, most of the lakes in the study area is connected to the stream of the Yangtze River and its branches. During the period of 1945-2013, there is no significant change and influence considered to be relevant with closed lakes.
- The current land cover map indicated the main land cover type replaced lakes is agricultural area, which have 70% of total former lakes. Then the forest holds 20%, and build-up area is less than 10%. This conclusion is derived from a large study area which covered half of Wuhan metropolitan area, and could not be deduced from the historical record which defines the urban expansion as the main driving factor of lake degradation in Wuhan city.

### 5.2. Recommendation

Lake is valuable resources which benefits ecological environment and human development. However, human activities have significant effects on the lake wetland area. The driving factor behind human activities have been analysed, which are indicated by the land cover map in this study. In order to further analysis the driving factor of lake changes, it is suggested to use more accurate and detailed land cover information. The reliability of the driving factor analysis will be more accurate if using the image of Sentinel satellite image, or the official land cover map from China government.



The combination of legacy map-derived and satellite-derived information provides a long-term evaluation of lakes in study area date back to the middle of 20th century, and this advantage should be better utilized. The process tree for legacy map extraction built in this study only provides a rough result, which still need manual correction. It is suggested to develop approaches to derive information from legacy maps automatically, which will allow the lake change assessment with series maps on larger extent.

## LIST OF REFERENCES

---

- Brönmark, C., & Hansson, L.-A. (2002). Environmental issues in lakes and ponds: current state and perspectives. *Environmental Conservation*, 29(3), 290–307. <http://doi.org/10.1017/S0376892902000218>
- Burbridge, P. R. (1994). Integrated planning and management of freshwater habitats, including wetlands. *Hydrobiologia*, 285(1–3), 311–322. <http://doi.org/10.1007/BF00005678>
- Chipman, J.W., L. G. O. and A. A. G. (2009). Remote sensing methods for lake management: A guide for resource managers and decision-makers. *For the United States Environmental Protection Agency*, 132.
- Cohen, J. (1960). A coefficient of agreement for nominal scales. *Educational and Psychological Measurement*, 20(1), 37–46.
- Congalton, R. G. (1991). A review of assessing the accuracy of classifications of remotely sensed data. *Remote Sensing of Environment*, 37(1), 35–46.
- Cui, L., Gao, C., Zhao, X., Ma, Q., Zhang, M., Li, W., ... Zhang, Y. (2013). Dynamics of the lakes in the middle and lower reaches of the Yangtze River basin, China, since late nineteenth century. *Environmental Monitoring and Assessment*, 185(5), 4005–4018. <http://doi.org/10.1007/s10661-012-2845-0>
- Deng, H. (2006). Quantitative analysis on the evolution of Jiangnan lakes region over the last 50 years. *Resources and Environment in the Yangtze Basin*, 15(2), 244–248.
- Detenbeck, N. a O. M. I. E., Taylor, D. E. B. R. a L., Lima, a N. N., & Hagley, C. (1995). Area : Implications for Monitoring Strategies and. *Environmental Monitoring and Assessment*, (1), 11–40.
- Dörnhöfer, K., & Oppelt, N. (2016). Remote sensing for lake research and monitoring - Recent advances. *Ecological Indicators*, 64, 105–122. <http://doi.org/10.1016/j.ecolind.2015.12.009>
- Fang, J., Wang, Z., Zhao, S., Li, Y., Tang, Z., Yu, D., ... Zheng, C. (2006). Biodiversity changes in the lakes of the Central Yangtze. *Frontiers in Ecology and the Environment*, 4(7), 369–377. [http://doi.org/10.1890/1540-9295\(2006\)004\[0369:BCITLO\]2.0.CO;2](http://doi.org/10.1890/1540-9295(2006)004[0369:BCITLO]2.0.CO;2)
- Fowler, B. (2000). A Sociological Analysis of the Satanic Verses Affair. *Theory, Culture & Society*, 17(1), 39–61. <http://doi.org/10.1177/02632760022050997>
- Gao, H. (2015). Satellite remote sensing of large lakes and reservoirs: from elevation and area to storage. *Wiley Interdisciplinary Reviews: Water*, 2(2), 147–157. <http://doi.org/10.1002/wat2.1065>
- Google Earth. (2017). Retrieved February 12, 2017, from <https://www.google.com/earth/>
- Groot, D. (2006). *Valuing wetlands. Water Management* (Vol. 455). Retrieved from [http://www.ramsar.org/pdf/lib/lib\\_rtr03.pdf](http://www.ramsar.org/pdf/lib/lib_rtr03.pdf)
- Huang, C., Peng, Y., Lang, M., Yeo, I.-Y., & McCarty, G. (2014). Wetland inundation mapping and change monitoring using Landsat and airborne LiDAR data. *Remote Sensing of Environment*, 141, 231–242. <http://doi.org/10.1016/j.rse.2013.10.020>
- Jiang, D., Fu, X., & Wang, K. (2013). Vegetation dynamics and their response to freshwater inflow and climate variables in the Yellow River Delta, China. *Quaternary International*, 304, 75–84.
- Jiang, H., Feng, M., Zhu, Y., Lu, N., Huang, J., & Xiao, T. (2014). An Automated Method for Extracting Rivers and Lakes from Landsat Imagery. *Remote Sensing*, 6(6), 5067–5089. <http://doi.org/10.3390/rs6065067>
- Kerle, N., & Leeuw, J. De. (2009). Object-Oriented Image Processing Techniques, 47(7), 2392–2402.
- Landis, J. R., & Koch, G. G. (1977). The measurement of observer agreement for categorical data. *Biometrics*, 159–174.
- Landsat Missions. (2017). Retrieved February 11, 2017, from <https://landsat.usgs.gov/what-are-band-designations-landsat-satellites>
- Lemly, A. D., & Ohlendorf, H. M. (2002). Regulatory Implications of Using Constructed Wetlands to Treat Selenium-Laden Wastewater. *Ecotoxicology and Environmental Safety*, 52(1), 46–56. <http://doi.org/10.1006/eesa.2002.2145>
- Levachkine, S., Velázquez, A., Alexandrov, V., & M. (2002). Semantic analysis and recognition of raster-scanned color cartographic images. *Graphics Recognition*, 178–189. Retrieved from <http://www.springerlink.com/index/v6pulyef4f1dlvqu.pdf>
- Liu, Z., Yao, Z., & Wang, R. (2016). Assessing methods of identifying open water bodies using Landsat 8 OLI imagery. *Environmental Earth Sciences*, 75(10), 873. <http://doi.org/10.1007/s12665-016-5686-2>
- Ma, R. H., Yang, G. S., Duan, H. T., Jiang, J. H., Wang, S. M., Feng, X. Z., ... Li, S. J. (2011). China's lakes at present: Number, area and spatial distribution. *Science China Earth Sciences*, 54(2), 283–289. <http://doi.org/10.1007/s11430-010-4052-6>

- Malahlela, O. E. (2016). Inland waterbody mapping: towards improving discrimination and extraction of inland surface water features. *International Journal of Remote Sensing*, 37(19), 4574–4589. <http://doi.org/10.1080/01431161.2016.1217441>
- McGarigal, K., Cushman, S., & Ene, E. (2012). FRAGSTATS v4: Spatial Pattern Analysis Program for Categorical and Continuous Maps. Retrieved from <http://www.umass.edu/landeco/research/fragstats/fragstats.html>
- Niu, Z., Zhang, H., Wang, X., Yao, W., Zhou, D., Zhao, K., ... Gong, P. (2012). Mapping wetland changes in China between 1978 and 2008. *Chinese Science Bulletin*, 57(22), 2813–2823. <http://doi.org/10.1007/s11434-012-5093-3>
- Pezeshk, A., & Tutwiler, R. L. (2011). Automatic feature extraction and text recognition from scanned topographic maps. *IEEE Transactions on Geoscience and Remote Sensing*, 49(12 PART 2), 5047–5063. <http://doi.org/10.1109/TGRS.2011.2157697>
- Rokni, K., Ahmad, A., Selamat, A., & Hazini, S. (2014). Water feature extraction and change detection using multitemporal landsat imagery. *Remote Sensing*, 6(5), 4173–4189. <http://doi.org/10.3390/rs6054173>
- Rokni, K., Ahmad, A., Solaimani, K., & Hazini, S. (2015). A new approach for surface water change detection: Integration of pixel level image fusion and image classification techniques. *International Journal of Applied Earth Observation and Geoinformation*, 34(1), 226–234. <http://doi.org/10.1016/j.jag.2014.08.014>
- Skidmore, A. K. (1999). Accuracy assessment of spatial information. In *Spatial statistics for remote sensing* (pp. 197–209). Springer.
- Sun, F., Sun, W., Chen, J., & Gong, P. (2012). Comparison and improvement of methods for identifying waterbodies in remotely sensed imagery. *International Journal of Remote Sensing*, 33(21), 6854–6875. <http://doi.org/10.1080/01431161.2012.692829>
- Tang, C., Fan, J., & Sun, W. (2015). Distribution characteristics and policy implications of territorial development suitability of the Yangtze River Basin. *Journal of Geographical Sciences*, 25(11), 1377–1392. <http://doi.org/10.1007/s11442-015-1240-5>
- USGS.gov. (2016). Retrieved February 12, 2017, from <https://www.usgs.gov/>
- Wang, X., Ning, L., Yu, J., Xiao, R., & Li, T. (2008). Changes of urban wetland landscape pattern and impacts of urbanization on wetland in Wuhan City. *Chinese Geographical Science*, 18(1), 47–53. <http://doi.org/10.1007/s11769-008-0047-z>
- Xu, K., Kong, C., Liu, G., Wu, C., Deng, H., Zhang, Y., & Zhuang, Q. (2010). Changes of urban wetlands in Wuhan, China, from 1987 to 2005. *Progress in Physical Geography*, 34, 207–220. <http://doi.org/10.1177/0309133309360626>
- Xu, K., Kong, C., Wu, C., Liu, G., Deng, H., & Zhang, Y. (2009). Dynamic changes in Tangxunhu wetland over a period of rapid development (1953–2005) in Wuhan, China. *Wetlands*, 29(4), 1255–1261. <http://doi.org/10.1672/08-238.1>